

# Quark–antiquark states and their radiative transitions in terms of the spectral integral equation.

## I. Bottomonia

V.V. Anisovich, L.G. Dakhno, M.A. Matveev,  
V.A. Nikonov and A.V. Sarantsev

June 17, 2021

### Abstract

In the framework of the spectral integral equation, we consider the  $b\bar{b}$  states and their radiative transitions. We reconstruct the  $b\bar{b}$  interaction on the basis of data for the levels of the bottomonium states with  $J^{PC} = 0^{-+}, 1^{--}, 0^{++}, 1^{++}, 2^{++}$  as well as the data for the radiative transitions  $\Upsilon(3S) \rightarrow \gamma\chi_{bJ}(2P)$  and  $\Upsilon(2S) \rightarrow \gamma\chi_{bJ}(1P)$  with  $J = 0, 1, 2$ . We calculate bottomonium levels with the radial quantum numbers  $n \leq 6$ , their wave functions and corresponding radiative transitions. The ratios  $Br[\chi_{bJ}(2P) \rightarrow \gamma\Upsilon(2S)]/Br[\chi_{bJ}(2P) \rightarrow \gamma\Upsilon(1S)]$  for  $J = 0, 1, 2$  are found in the agreement with data. We determine the  $b\bar{b}$  component of the photon wave function using the data for the  $e^+e^-$  annihilation,  $e^+e^- \rightarrow \Upsilon(9460), \Upsilon(10023), \Upsilon(10036), \Upsilon(10580), \Upsilon(10865), \Upsilon(11019)$ , and predict partial widths of the two-photon decays  $\eta_{b0} \rightarrow \gamma\gamma, \chi_{b0} \rightarrow \gamma\gamma, \chi_{b2} \rightarrow \gamma\gamma$  for the radial excitation states below  $B\bar{B}$  threshold ( $n \leq 3$ ).

## 1 Introduction

In [1], see also [2], the program was suggested for the reconstruction of soft quark–antiquark interaction, on the basis of data on meson levels and meson radiative transitions. Now, we have the first results in the realization of this program for the  $b\bar{b}, c\bar{c}$  systems and light quarkonia  $q\bar{q}$ . In this paper we present the results for the bottomonia.

In [1], the equations for  $q\bar{q}$  systems were written in terms of the spectral integral representation. The spectral integration technique is precisely advantageous for composite particles, for the content of a composite system is thus strictly controlled and there is no problem with the description of high spin states. The equation for the composite  $q\bar{q}$  system in the spectral integration technique [1] is a direct generalization of the dispersion  $N/D$  equation, when we represent the  $N$ -function as a sum of separable vertices. In [1], this equation was conventionally called the spectral integral Bethe–Salpeter equation. However, it should be emphasized that

in certain important points it differs from the standard Bethe–Salpeter equation [3] written in the Feynman technique (the application of the Feynman technique to the calculation of meson states may be found, for example, in [4, 5, 6, 7, 8] and references therein).

The strong QCD is responsible for the formation of composite systems, though, despite a remarkable progress in this field, certain features of the soft interaction of color objects are rather enigmatic till now. A fascinating feature of the light quark ( $q = u, d, s$ ) meson spectra is the linearity of their trajectories on both the  $(J, M^2)$ - and  $(n, M^2)$ -planes ( $J$  is the spin of the  $q\bar{q}$  system with the mass  $M$  and  $n$  is its radial quantum number) [2, 9]. The linearity of trajectories has been also seen in the baryon sector [2, 10] — this fact allows one to suggest a specific role of diquarks in baryon systems, see the discussion in [2, 10] and references therein. Unfortunately, the number of experimentally observed excited states for baryons is much less than that given by the standard quark model calculation (e.g., see [11]) that limits our understanding of the three-quark interactions.

In practice, all the observed highly excited meson states (with  $M > 1500$  MeV) are lying on linear  $q\bar{q}$  trajectories, and we have no candidates for the  $q\bar{q}g$  hybrids. The effective gluon  $g$  has the mass  $m_g$  of the order of  $m_g \simeq 700 - 1000$  MeV, [12, 13, 14, 15], so the hybrid mesons could be spread over the region  $1500 - 2000$  MeV. Still, the experiment does not point to the increase of the meson state density in this region. Also, there are no definite indications to the existence of mesons with the exotic quantum numbers inherent in hybrids [16].

The particulars of hadron mass spectra discussed above point to the fact that in studying mesons in the soft region (or formed at large distances) the most reliable way is to consider the quark–antiquark interaction by determining their characteristics from the data. It is the guideline in our approach to the quark–antiquark systems.

The spectral integral equation [1] gives us a unique solution for the quark–antiquark levels and their wave functions, provided the interquark interaction is known. Let us emphasize that the equations work for both instantaneous interactions (or those of the potential type) and the  $t$ -channel exchanges with retardation, and even for the energy-dependent interactions: this follows from the fact that the equations themselves are the modified dispersion relations for the amplitude. For solving the inverse problem, that is, for reconstructing the interaction, it is not enough to know the meson masses — one should know the wave functions of quark–antiquark systems. Such an information is contained in the hadronic form factors and partial widths of radiative decays. Therefore, in the present approach, we consider simultaneously the meson spectra in terms of the spectral integral equations and meson radiative transitions in terms of the dispersion relations over meson masses — in this way, all the calculations are carried out within compatible methods.

The method of calculation of the radiative transition amplitudes in terms of the double dispersive integrals was developed in a number of papers [17, 18, 19]. An important point was the representation of the transition amplitude in the form convenient for simultaneous fitting to the spectral integral equation — it was done in [20, 21].

A significant information on the quark–antiquark meson wave functions is hidden in the two-photon meson decays:  $meson \rightarrow \gamma\gamma$ . For the calculation of such processes, one needs to

know the quark wave function of the photon; the method of reconstruction of the  $\gamma \rightarrow q\bar{q}$  and  $\gamma \rightarrow c\bar{c}$  vertices was developed in [22, 23].

The paper is organized as follows.

In Section 2, we present the technique and basic formulas which were used in fitting to quark–antiquark states. Here, we briefly recall the spectral integral equation and give the formulas for the radiative transition amplitudes of quark systems calculated within the double spectral integrals. Keeping in mind the application of these formulas to the other quark systems, we do not specify the flavor of the considered quark:  $(Q\bar{Q})_{in} \rightarrow \gamma + (Q\bar{Q})_{out}$ ,  $e^+e^- \rightarrow V(Q\bar{Q})$  and  $Q\bar{Q}$ -meson  $\rightarrow \gamma\gamma$ .

In Section 3, we consider the bottomonium systems: the choice of the  $b\bar{b}$ -mesons as a primary object for the study is motivated by the large  $b$ -quark mass, so the nonrelativistic approximation is expected to work well, and we can reliably compare our results with those obtained within nonrelativistic approaches [24, 25, 26, 27]. Different variants of the interaction (instantaneous and retarded) are discussed. The results of fitting to masses and radiative transitions (for both observed and predicted states) are presented and discussed. In the  $b\bar{b}$  sector, we reconstruct the interaction, on the basis of data on the levels of bottomonia with  $J^{PC} = 0^{-+}, 1^{--}, 0^{++}, 1^{++}, 2^{++}$  and radiative transitions  $\Upsilon(3S) \rightarrow \gamma\chi_{bJ}(2P)$  and  $\Upsilon(2S) \rightarrow \gamma\chi_{bJ}(1P)$  at  $J = 0, 1, 2$ . We calculate the bottomonium levels with radial quantum numbers  $n \leq 6$ , as well as their wave functions and corresponding radiative transitions. We determine the  $b\bar{b}$  component of the photon wave function on the basis of data for the  $e^+e^-$  annihilation reactions  $e^+e^- \rightarrow \Upsilon(9460), \Upsilon(10023), \Upsilon(10036), \Upsilon(10580), \Upsilon(10865), \Upsilon(11019)$ , and predict partial widths of the two-photon decays  $\eta_{b0} \rightarrow \gamma\gamma$ ,  $\chi_{b0} \rightarrow \gamma\gamma$ ,  $\chi_{b2} \rightarrow \gamma\gamma$  for the excited states with  $n \leq 3$ .

Brief summary is given in Conclusion.

## 2 Spectral integral equation and radiative transition amplitudes

Here we present the formulas used in fitting to the  $b\bar{b}$  systems. Of course, they may be also applied for the charmonia, as well as for light quark states  $q\bar{q}$  with  $I = 1$ , or one-flavor states with  $I = 0$  (pure  $s\bar{s}$  or  $n\bar{n} = (u\bar{u} + d\bar{d})/\sqrt{2}$  systems).

### 2.1 Spectral integral equation

The wave function of the quark–antiquark meson with the mass  $M$  is characterized by the total momentum  $J$ , quark–antiquark spin  $S$  (in the flavor nonet with fixed  $J^P$ , the values  $S = 0, 1$  determine  $C$  parity) and radial number  $n$ . We denote the wave function as  $\widehat{\Psi}_{(n)\mu_1\dots\mu_J}^{(S,J)}(k_\perp)$ , with  $k_\perp$  being relative quark momentum and the indices  $\mu_1, \dots, \mu_J$  related to the total momentum. For the heavy-quark  $Q\bar{Q}$  system, the spectral integral equation reads [1]:

$$(s - M^2) \widehat{\Psi}_{(n)\mu_1\dots\mu_J}^{(S,J)}(k_\perp) = \tag{1}$$

$$= \int_{4m^2}^{\infty} \frac{ds'}{\pi} \int d\Phi_2(P'; k'_1, k'_2) \widehat{V}(s, s', (k_{\perp} k'_{\perp})) (\widehat{k}'_1 + m) \widehat{\Psi}_{(n)\mu_1 \dots \mu_J}^{(S, J)}(k'_{\perp}) (-\widehat{k}'_2 + m).$$

Here, the quarks are mass-on-shell,  $k_1^2 = k_1'^2 = k_2^2 = k_2'^2 = m^2$ . The phase space factor in the intermediate state is determined as follows:

$$d\Phi_2(P'; k'_1, k'_2) = \frac{1}{2} \frac{d^3 k'_1}{(2\pi)^3 2k'_{10}} \frac{d^3 k'_2}{(2\pi)^3 2k'_{20}} (2\pi)^4 \delta^{(4)}(P' - k'_1 - k'_2). \quad (2)$$

The following notations are used:

$$k_{\perp} = \frac{1}{2}(k_1 - k_2), \quad P = k_1 + k_2, \quad k'_{\perp} = \frac{1}{2}(k'_1 - k'_2), \quad P' = k'_1 + k'_2, \quad (3)$$

$$P^2 = s, \quad P'^2 = s', \quad g_{\mu\nu}^{\perp} = g_{\mu\nu} - \frac{P_{\mu} P_{\nu}}{s}, \quad g_{\mu\nu}^{\prime\perp} = g_{\mu\nu} - \frac{P'_{\mu} P'_{\nu}}{s'},$$

so one can write  $k_{\mu}^{\perp} = k_{\nu} g_{\nu\mu}^{\perp}$  and  $k_{\mu}^{\prime\perp} = k'_{\nu} g_{\nu\mu}^{\prime\perp}$ . In the center-of-mass system, the integration can be re-written as

$$\int_{4m^2}^{\infty} \frac{ds'}{\pi} \int d\Phi_2(P'; k'_1, k'_2) \longrightarrow \int \frac{d^3 k'}{(2\pi)^3 k'_0}, \quad (4)$$

where  $k'$  is the momentum of one of the quarks.

For the fermion–antifermion system with definite  $J, S$  and  $L$  (angular momentum), we introduce the moment operators  $Q_{\mu_1 \dots \mu_J}^{(S, L, J)}(k_{\perp})$  defined as follows [28]:

$$Q_{\mu_1 \mu_2 \dots \mu_J}^{(0, J, J)}(k_{\perp}) = i\gamma_5 X_{\mu_1 \dots \mu_J}(k_{\perp}) \sqrt{\frac{2J+1}{\alpha_J}}, \quad (5)$$

$$Q_{\mu_1 \dots \mu_J}^{(1, J, J)}(k_{\perp}) = \frac{i\varepsilon_{\alpha\eta\xi\gamma} \gamma_{\eta} k_{\xi}^{\perp} P_{\gamma} Z_{\mu_1 \dots \mu_J}^{\alpha}}{\sqrt{s}} \sqrt{\frac{(2J+1)J}{(J+1)\alpha_J}},$$

$$Q_{\mu_1 \dots \mu_J}^{(1, J+1, J)}(k_{\perp}) = \gamma_{\alpha} X_{\alpha\mu_1 \dots \mu_J} \sqrt{\frac{J+1}{\alpha_J}},$$

$$Q_{\mu_1 \dots \mu_J}^{(1, J-1, J)}(k_{\perp}) = \gamma_{\alpha} Z_{\mu_1 \dots \mu_J}^{\alpha} \sqrt{\frac{J}{\alpha_J}}, \quad (6)$$

where  $\alpha_J = (2J-1)!!/J!$  and

$$\begin{aligned} X_{\mu_1 \dots \mu_J}^{(J)}(k_{\perp}) = & \frac{(2J-1)!!}{J!} \left[ k_{\mu_1}^{\perp} k_{\mu_2}^{\perp} k_{\mu_3}^{\perp} k_{\mu_4}^{\perp} \dots k_{\mu_J}^{\perp} - \right. \\ & - \frac{k_{\perp}^2}{2J-1} \left( g_{\mu_1 \mu_2}^{\perp} k_{\mu_3}^{\perp} k_{\mu_4}^{\perp} \dots k_{\mu_J}^{\perp} + g_{\mu_1 \mu_3}^{\perp} k_{\mu_2}^{\perp} k_{\mu_4}^{\perp} \dots k_{\mu_J}^{\perp} + \dots \right) + \\ & + \frac{k_{\perp}^4}{(2J-1)(2J-3)} \left( g_{\mu_1 \mu_2}^{\perp} g_{\mu_3 \mu_4}^{\perp} k_{\mu_5}^{\perp} k_{\mu_6}^{\perp} \dots k_{\mu_J}^{\perp} + \right. \\ & \left. + g_{\mu_1 \mu_2}^{\perp} g_{\mu_3 \mu_5}^{\perp} k_{\mu_4}^{\perp} k_{\mu_6}^{\perp} \dots k_{\mu_J}^{\perp} + \dots \right) + \dots \left. \right], \quad (7) \end{aligned}$$

$$Z_{\mu_1 \dots \mu_J, \alpha}^{(J-1)}(k_\perp) = \frac{2J-1}{J^2} \left( \sum_{i=1}^J X_{\mu_1 \dots \mu_{i-1} \mu_{i+1} \dots \mu_J}^{(J-1)}(k_\perp) g_{\mu_i \alpha}^\perp - \frac{2}{2J-1} \sum_{\substack{i,j=1 \\ i < j}}^J g_{\mu_i \mu_j}^\perp X_{\mu_1 \dots \mu_{i-1} \mu_{i+1} \dots \mu_{j-1} \mu_{j+1} \dots \mu_J \alpha}^{(J-1)}(k_\perp) \right).$$

The operators are normalized as:

$$\begin{aligned} \int \frac{d\Omega}{4\pi} \text{Sp}[Q_{\mu_1 \dots \mu_L}^{(0,J,J)}(m + \hat{k}_1) Q_{\nu_1 \dots \nu_L}^{(0,J,J)}(m - \hat{k}_2)] &= -2s \mathbf{k}^{2J} (-1)^J O_{\nu_1 \dots \nu_J}^{\mu_1 \dots \mu_J}, \\ \int \frac{d\Omega}{4\pi} \text{Sp}[Q_{\mu_1 \dots \mu_J}^{(1,J,J)}(m + \hat{k}_1) Q_{\nu_1 \dots \nu_J}^{(1,J,J)}(m - \hat{k}_2)] &= -2s \mathbf{k}^{2J} (-1)^J O_{\nu_1 \dots \nu_J}^{\mu_1 \dots \mu_J}, \\ \int \frac{d\Omega}{4\pi} \text{Sp}[Q_{\mu_1 \dots \mu_n}^{(1,J+1,J)}(m + \hat{k}_1) Q_{\nu_1 \dots \nu_J}^{(1,J+1,J)}(m - \hat{k}_2)] &= \left( \frac{8(J+1)\mathbf{k}^2}{2J+1} - 2s \right) \mathbf{k}^{2(J+1)} (-1)^J O_{\nu_1 \dots \nu_J}^{\mu_1 \dots \mu_J}, \\ \int \frac{d\Omega}{4\pi} \text{Sp}[Q_{\mu_1 \dots \mu_J}^{(1,J-1,J)}(m + \hat{k}_1) Q_{\nu_1 \dots \nu_J}^{(1,J-1,J)}(m - \hat{k}_2)] &= \left( \frac{8J\mathbf{k}^2}{2J+1} - 2s \right) \mathbf{k}^{2(J-1)} (-1)^J O_{\nu_1 \dots \nu_J}^{\mu_1 \dots \mu_J}, \\ \int \frac{d\Omega}{4\pi} \text{Sp}[Q_{\mu_1 \dots \mu_J}^{(1,J-1,J)}(m + \hat{k}_1) Q_{\nu_1 \dots \nu_J}^{(1,J+1,J)}(m - \hat{k}_2)] &= -8 \frac{\sqrt{J(J+1)}}{2J+1} \mathbf{k}^{2(J+1)} (-1)^J O_{\nu_1 \dots \nu_J}^{\mu_1 \dots \mu_J}. \end{aligned} \quad (8)$$

Here,  $O_{\nu_1 \dots \nu_n}^{\mu_1 \dots \mu_n}$  is the projection operator to a state with the momentum  $J$  and  $s = 4m^2 + 4\vec{k}^2$ . The projection operators have the following properties:

$$X_{\mu_1 \dots \mu_L}^{(L)}(k_\perp) O_{\nu_1 \dots \nu_L}^{\mu_1 \dots \mu_L} = X_{\nu_1 \dots \nu_L}^{(L)}(k_\perp), \quad O_{\alpha_1 \dots \alpha_L}^{\mu_1 \dots \mu_L} O_{\nu_1 \dots \nu_L}^{\alpha_1 \dots \alpha_L} = O_{\nu_1 \dots \nu_L}^{\mu_1 \dots \mu_L}. \quad (9)$$

Let us underline that  $(-1)^J O_{\nu_1 \dots \nu_J}^{\mu_1 \dots \mu_J}$  describes the spin structure of the propagator of a particle with the total spin  $J$  (see [28] for more detail).

In terms of these operators, the wave functions read:

$$\widehat{\Psi}_{(n) \mu_1 \dots \mu_J}^{(S,J)}(k_\perp) = Q_{\mu_1 \dots \mu_J}^{(S,J,J)}(k_\perp) \psi_n^{(S,L=J,J)}(k_\perp^2), \quad S = 0, 1 \text{ and } J = L, \quad (10)$$

$$\widehat{\Psi}_{(n) \mu_1 \dots \mu_J}^{(S,J)}(k_\perp) = Q_{\mu_1 \dots \mu_J}^{(S,J+1,J)}(k_\perp) \psi_n^{(S,L=J+1,J)}(k_\perp^2) + Q_{\mu_1 \dots \mu_J}^{(S,J-1,J)}(k_\perp) \psi_n^{(S,L=J-1,J)}(k_\perp^2), \quad J \neq L,$$

where the functions  $\psi_n^{(S,L,J)}(k_\perp^2)$  depend on  $k_\perp^2$  only (recall that in the center-of-mass system  $k_\perp^2 = -\mathbf{k}^2$ ).

The wave functions with  $L = J$  are normalized as follows:

$$1 = \int \frac{d^3k}{(2\pi^3)k_0} 2s |\mathbf{k}|^{2J} |\psi_n^{(S,L=J,J)}(k_\perp^2)|^2, \quad (11)$$

while for  $L = J \pm 1$  the normalization reads:

$$\begin{aligned} 1 &= \int \frac{d^3k}{(2\pi^3)k_0} |\psi_n^{(S,J+1,J)}(k_\perp^2)|^2 \left( 2s - \frac{8(J+1)\mathbf{k}^2}{2J+1} \right) \mathbf{k}^{2(J+1)} + \\ &+ 16 \frac{\sqrt{J(J+1)}}{2J+1} \mathbf{k}^{2(J+1)} \psi_n^{(S,J+1,J)}(k_\perp^2) \psi_n^{*(S,J-1,J)}(k_\perp^2) + |\psi_n^{(S,J-1,J)}(k_\perp^2)|^2 \left( 2s - \frac{8J\mathbf{k}^2}{2J+1} \right) \mathbf{k}^{2(J-1)}. \end{aligned} \quad (12)$$

We re-write this normalization condition as follows:

$$W_{J+1,J+1} + W_{J+1,J-1} + W_{J-1,J-1} = 1, \quad (13)$$

where  $W_{J+1,J+1}$ ,  $W_{J+1,J-1}$  and  $W_{J-1,J-1}$  are determined by the wave function convolutions  $(\psi_n^{(S,J+1,J)}\psi_n^{(S,J+1,J)})$ ,  $(\psi_n^{(S,J+1,J)}\psi_n^{(S,J-1,J)})$  and  $(\psi_n^{(S,J-1,J)}\psi_n^{(S,J-1,J)})$ , correspondingly.

The interaction block can be expanded in a series with respect to a full set of the  $t$ -channel operators  $\hat{O}_I$ :

$$\begin{aligned} \hat{O}_I &= \mathbf{I}, \quad \gamma_\mu, \quad i\sigma_{\mu\nu}, \quad i\gamma_\mu\gamma_5, \quad \gamma_5, \\ \hat{V}(s, s', (k_\perp k'_\perp)) &= \sum_I V_I(s, s', (k_\perp k'_\perp)) \hat{O}_I \otimes \hat{O}_I, \end{aligned} \quad (14)$$

By solving the equation, the  $t$ -channel operators should be transformed in the two  $s$ -channel ones; this procedure is clarified in Appendix I.

The equation (1) is written in the momentum representation, and we solve it in the momentum representation too. The equation (1) allows one to use as an interaction the instantaneous approximation, or take into account the retardation effects. In the instantaneous approximation one has

$$\hat{V}(s, s', (k_\perp k'_\perp)) \longrightarrow \hat{V}(t_\perp), \quad t_\perp = (k_{1\perp} - k'_{1\perp})_\mu (-k_{2\perp} + k'_{2\perp})_\mu. \quad (15)$$

The retardation effects are taken into account, when the momentum transfer squared  $t$  in the interaction block depends on the time components of the quark momentum (for more detail see Section 2.5 of [1] and the discussion in: [29, 30, 31, 32]):

$$\hat{V}(s, s', (k_\perp k'_\perp)) \longrightarrow \hat{V}(t), \quad t = (k_1 - k'_1)_\mu (-k_2 + k'_2)_\mu. \quad (16)$$

Fitting to quark-antiquark states, we use the interaction blocks with the following  $t$ -dependence:

$$\begin{aligned} I_{-1} &= \frac{4\pi}{\mu^2 - t}, \\ I_0 &= \frac{8\pi\mu}{(\mu^2 - t)^2}, \\ I_1 &= 8\pi \left( \frac{4\mu^2}{(\mu^2 - t)^3} - \frac{1}{(\mu^2 - t)^2} \right), \\ I_2 &= 96\pi\mu \left( \frac{2\mu^2}{(\mu^2 - t)^4} - \frac{1}{(\mu^2 - t)^3} \right), \\ I_3 &= 96\pi \left( \frac{16\mu^4}{(\mu^2 - t)^5} - \frac{12\mu^2}{(\mu^2 - t)^4} + \frac{1}{(\mu^2 - t)^3} \right), \end{aligned} \quad (17)$$

or in general case

$$I_N = \frac{4\pi(N+1)!}{(\mu^2 - t)^{N+2}} \sum_{n=0}^{N+1} (\mu + \sqrt{t})^{N+1-n} (\mu - \sqrt{t})^n. \quad (18)$$

Traditionally, the interaction of heavy quarks in the instantaneous approximation is represented in terms of the potential  $V(r)$ . The form of the potential can be obtained with the Fourier

transform of (17) in the center-of-mass system. Thus, we have

$$\begin{aligned} t_{\perp} &= -(\vec{k} - \vec{k}')^2 = -\vec{q}^2, \\ I_N^{(coord)}(r, \mu) &= \int \frac{d^3q}{(2\pi)^3} e^{-i\vec{q}\vec{r}} I_N(t_{\perp}), \end{aligned} \quad (19)$$

that gives

$$I_N^{(coord)}(r, \mu) = r^N e^{-\mu r}. \quad (20)$$

Working with the instantaneous interaction, we consider the following types of  $V(r)$ :

$$V(r) = a + b r + c e^{-\mu_c r} + d \frac{e^{-\mu_d r}}{r}, \quad (21)$$

where the constant and linear (confinement) terms read:

$$\begin{aligned} a &\rightarrow a I_0^{(coord)}(r, \mu_{constant} \rightarrow 0), \\ br &\rightarrow b I_1^{(coord)}(r, \mu_{linear} \rightarrow 0). \end{aligned} \quad (22)$$

The limits  $\mu_{constant} \mu_{linear} \rightarrow 0$  mean that in the fitting procedure the parameters  $\mu_{constant}$  and  $\mu_{linear}$  are chosen to be small enough, of the order of 1–10 MeV. It was checked that the solution for the states with  $n \leq 6$  is stable, when  $\mu_{constant}$  and  $\mu_{linear}$  change in this interval.

### 2.1.1 Wave functions

Let us present in the explicit form the wave functions of the studying states:  $0^{-+}$ ,  $1^{--}$ ,  $0^{++}$ ,  $1^{++}$ ,  $2^{++}$ ,  $1^{+-}$ . The wave functions of these states,  $\hat{\Psi}_{(n)\mu_1, \mu_2, \dots, \mu_J}^{(S, J)}$ , in terms of the operators (5) and invariant functions  $\psi_n^{(S, L, J)}(k_{\perp}^2)$  read:

$$\begin{aligned} 0^{-+} : \quad & \hat{\Psi}_{(n)}^{(0,0)} = i\gamma_5 \psi_n^{(0,0,0)}(k^2), \\ 1^{--} : \quad & \hat{\Psi}_{(n)\mu}^{(1,1)} = \gamma_{\mu}^{\perp} \psi_n^{(1,0,1)}(k^2) + \frac{3}{\sqrt{2}} \left[ k_{\mu} \hat{k} - \frac{1}{3} k^2 \gamma_{\mu}^{\perp} \right] \psi_n^{(1,2,1)}(k^2), \\ 0^{++} : \quad & \hat{\Psi}_{(n)}^{(1,0)} = m I \psi_n^{(1,1,0)}(k^2), \\ 1^{++} : \quad & \hat{\Psi}_{(n)\mu}^{(1,1)} = \sqrt{\frac{3}{2s}} i \varepsilon_{\gamma P k \mu} \psi_n^{(1,1,1)}(k^2), \\ 2^{++} : \quad & \hat{\Psi}_{(n)\mu_1 \mu_2}^{(1,2)} = \sqrt{\frac{3}{4}} \left[ k_{\mu_1} \gamma_{\mu_2}^{\perp} + k_{\mu_2} \gamma_{\mu_1}^{\perp} - \frac{2}{3} \hat{k} g_{\mu_1 \mu_2}^{\perp} \right] \psi_n^{(1,1,2)}(k^2) + \\ & + \frac{5}{\sqrt{2}} \left[ k_{\mu_1} k_{\mu_2} \hat{k} - \frac{1}{5} k^2 (g_{\mu_1 \mu_2}^{\perp} \hat{k} + \gamma_{\mu_1}^{\perp} k_{\mu_2} + k_{\mu_1} \gamma_{\mu_2}^{\perp}) \right] \psi_n^{(1,3,2)}(k^2), \\ 1^{+-} : \quad & \hat{\Psi}_{(n)\mu}^{(0,1)} = \sqrt{3} i \gamma_5 k_{\mu} \psi_n^{(0,1,1)}(k^2). \end{aligned} \quad (23)$$

Here, the short notations are used  $k^{\perp} \equiv k = (k_1 - k_2)/2$  ( $(kP) = 0$  at quark masses equal to each other) and  $\varepsilon_{\gamma P k \mu} \equiv \varepsilon_{\nu_1 \nu_2 \nu_3 \mu} \gamma_{\nu_1} P_{\nu_2} k_{\nu_3}$  as well as the equality  $\hat{k} = mI$  (recall again that in the spectral integral technique the constituents are mass-on-shell).

The  $1^{--}$  and  $2^{++}$  states are defined by two wave functions with different  $L$ ; correspondingly, there are two wave functions for these two levels.

The  $1^{--}$  state is characterized by two angular momenta,  $L = 0$  and  $L = 2$ . The states in (23) are not pure with respect to  $L$ , for the wave function  $\gamma_\mu^\perp \psi^{(1,0,1)}(k^2)$  is a mixture of  $S$ - and  $D$ -waves. The pure  $S$  state is given by the following operator (e.g., see [17, 21]):

$$\Gamma_\mu = \gamma_\mu^\perp - \frac{k_\mu}{2m + \sqrt{s}}. \quad (24)$$

In the nonrelativistic limit, the operators  $\Gamma_\mu$  and  $\gamma_\mu^\perp$  coincide:  $[\Gamma_\mu \simeq \gamma_\mu^\perp]_{nonrel}$ . Likewise, the pure  $P$  state of the system  $2^{++}$  is defined by the following operator [21]:

$$T_{\mu_1\mu_2} = \sqrt{\frac{3}{4}} \left[ k_{\mu_1} \Gamma_{\mu_2} + k_{\mu_2} \Gamma_{\mu_1} - \frac{2}{3} (k\Gamma) g_{\mu_1\mu_2}^\perp \right]. \quad (25)$$

Note that for heavy quarks the use of pure operators (24), (25) results in the insignificant modification of the wave function representation, for the  $\gamma_\mu^\perp$  operator leads to a small admixture of the  $D$ -wave and, vice versa, the  $\frac{3}{\sqrt{2}} [k_\mu \hat{k} - \frac{1}{3} k^2 \gamma_\mu^\perp]$  operator results in a state with dominant  $D$ -wave, with a small admixture of the  $S$ -wave. Similarly, for the state  $2^{++}$  the operator  $\sqrt{\frac{3}{4}} [k_{\mu_1} \gamma_{\mu_2}^\perp + k_{\mu_2} \gamma_{\mu_1}^\perp - \frac{2}{3} \hat{k} g_{\mu_1\mu_2}^\perp]$  leads to the dominant  $P$ -wave, while the operator  $\frac{5}{\sqrt{2}} [k_{\mu_1} k_{\mu_2} \hat{k} - \frac{1}{5} k^2 (g_{\mu_1\mu_2}^\perp \hat{k} + \gamma_{\mu_1}^\perp k_{\mu_2} + k_{\mu_1} \gamma_{\mu_2}^\perp)]$  gives us the dominant  $F$ -wave.

Let us note that dealing with the operators of pure states, like (24) and (25), would not facilitate the fitting procedure, for real states are the mixture of different waves ( $S$ ,  $D$  for  $1^{--}$  and  $P$ ,  $F$  for  $2^{++}$ ).

## 2.2 Radiative transitions $(Q\bar{Q})_{in} \rightarrow \gamma(Q\bar{Q})_{out}$

Here, we list the formulas for the amplitudes and partial widths of the radiative transitions  $(Q\bar{Q})_{in} \rightarrow \gamma(Q\bar{Q})_{out}$  used in the fit. The technique for the calculation of the transition amplitudes  $(Q\bar{Q})_{in} \rightarrow \gamma(Q\bar{Q})_{out}$  was developed in [18, 19, 20, 21]. In [33], the transition form factors were transformed to the form convenient for the fitting procedure, and we present them in this form below.

### 2.2.1 Transitions of the vector ( $1^{--}$ ) and pseudoscalar ( $0^{-+}$ ) mesons

Here, we present the formulas for the radiative transitions of the vector ( $V$ ) and pseudoscalar ( $P$ ) mesons. The partial widths for the decays  $V \rightarrow \gamma P$  and  $P \rightarrow \gamma V$  read:

$$\begin{aligned} M_V \Gamma_{V \rightarrow \gamma P} &= \frac{1}{24} \alpha \frac{(M_V^2 - M_P^2)^3}{M_V^2} |F_{V \rightarrow \gamma P}|^2, \\ M_P \Gamma_{P \rightarrow \gamma V} &= \frac{1}{8} \alpha \frac{(M_P^2 - M_V^2)^3}{M_P^2} |F_{V \rightarrow \gamma P}|^2, \end{aligned} \quad (26)$$



where  $\alpha = e^2/4\pi = 1/137$ . The transition form factor is expressed in terms of the  $Q\bar{Q}$  wave functions  $\psi_n^{(0,0,0)}(k^2)$  and  $\psi_n^{(1,0,1)}(k^2)$ , see (23). However, in line with [19, 20, 21], we change the notations as follows:

$$\psi_n^{(0,0,0)}(k^2) \equiv \psi_P(s), \quad \psi_n^{(1,0,1)}(k^2) \equiv \psi_{V(0)}(s), \quad \psi_n^{(1,2,1)}(k^2) \equiv \psi_{V(2)}(s). \quad (27)$$

In terms of  $\psi_V(s)$  and  $\psi_P(s)$ , the form factors are written as:

$$F_{V(0) \rightarrow \gamma P} = Z_{V \rightarrow \gamma P} \frac{m}{4\pi} \int_{4m^2}^{\infty} \frac{ds}{\pi} \psi_{V(0)}(s) \psi_P(s) \ln \frac{\sqrt{s} + \sqrt{s - 4m^2}}{\sqrt{s} - \sqrt{s - 4m^2}}, \quad (28)$$

$$F_{V(2) \rightarrow \gamma P} = Z_{V \rightarrow \gamma P} \frac{m}{32\sqrt{2}\pi} \int_{4m^2}^{\infty} \frac{ds}{\pi} \psi_{V(2)}(s) \psi_P(s) \times \quad (29)$$

$$\times \left[ (2m^2 + s) \ln \frac{\sqrt{s} + \sqrt{s - 4m^2}}{\sqrt{s} - \sqrt{s - 4m^2}} - 3\sqrt{s(s - 4m^2)} \right],$$

where  $Z_{V \rightarrow \gamma P}$  is the charge factor:

$$Z_{V \rightarrow \gamma P} = 2e_Q, \quad e_c = \frac{2}{3}, \quad e_b = -\frac{1}{3}. \quad (30)$$

The total transition form factor reads:

$$F_{V \rightarrow \gamma P} = F_{V(0) \rightarrow \gamma P} + F_{V(2) \rightarrow \gamma P}. \quad (31)$$

Normalization conditions are determined by Eq. (12), they can be written, after the integration over the angle variables, as the integrals over  $s$ :

$$\int \frac{d^3k}{(2\pi^3)k_0} \rightarrow \int_{4m^2}^{\infty} \frac{ds}{16\pi^2} \sqrt{\frac{s - 4m^2}{s}}. \quad (32)$$

Normalization conditions for vector state determined by Eq. (12) read:

$$1 = W_{00}[V] + W_{02}[V] + W_{22}[V], \quad (33)$$

$$W_{00}[V] = \frac{1}{3} \int_{4m^2}^{\infty} \frac{ds}{16\pi^2} \psi_{V(0)}^2(s) 4(s + 2m^2) \sqrt{\frac{s - 4m^2}{s}}, \quad (34)$$

$$W_{02}[V] = \frac{\sqrt{2}}{3} \int_{4m^2}^{\infty} \frac{ds}{16\pi^2} \psi_{V(0)}(s) \psi_{V(2)}(s) (s - 4m^2)^2 \sqrt{\frac{s - 4m^2}{s}},$$

$$W_{22}[V] = \frac{2}{3} \int_{4m^2}^{\infty} \frac{ds}{16\pi^2} \psi_{V(2)}^2(s) \frac{(8m^2 + s)(s - 4m^2)^2}{16} \sqrt{\frac{s - 4m^2}{s}}.$$

Normalization condition for  $\psi_P(s)$  in the  $s$ -integral representation is:

$$1 = \int_{4m^2}^{\infty} \frac{ds}{16\pi^2} \psi_P^2(s) 2s \sqrt{\frac{s - 4m^2}{s}}. \quad (35)$$

### 2.2.2 Transitions of the vector ( $1^{--}$ ) and scalar ( $0^{++}$ ) mesons

The partial widths of the vector ( $V$ ) and scalar ( $S$ ) meson decays,  $V \rightarrow \gamma S$  and  $S \rightarrow \gamma V$ , read:

$$\begin{aligned} M_V \Gamma_{V \rightarrow \gamma S} &= \frac{1}{6} \alpha \frac{M_V^2 - M_S^2}{M_V^2} |F_{V \rightarrow \gamma S}|^2, \\ M_S \Gamma_{S \rightarrow \gamma V} &= \frac{1}{2} \alpha \frac{M_S^2 - M_V^2}{M_S^2} |F_{V \rightarrow \gamma S}|^2. \end{aligned} \quad (36)$$

The transition form factor  $F_{V \rightarrow \gamma S}$  is expressed in terms of the wave functions  $\psi_n^{(1,0,1)}(k^2)$ ,  $\psi_n^{(1,2,1)}(k^2)$  and  $\psi_n^{(1,1,0)}(k^2)$ . Changing the notation in line with, [19, 20, 21]

$$\psi_n^{(1,1,0)}(k^2) \equiv \psi_S(s), \quad (37)$$

we have:

$$\begin{aligned} F_{V(0) \rightarrow \gamma S} &= Z_{V \rightarrow \gamma S} \frac{m^2}{4\pi} \int_{4m^2}^{\infty} \frac{ds}{\pi} \psi_{V(0)}(s) \psi_S(s) I_{V \rightarrow \gamma S}(s), \\ F_{V(2) \rightarrow \gamma S} &= Z_{V \rightarrow \gamma S} \frac{\sqrt{2}m^2}{16\pi} \int_{4m^2}^{\infty} \frac{ds}{\pi} \psi_{V(2)}(s) \psi_S(s) (-s + 4m^2) I_{V \rightarrow \gamma S}(s), \\ I_{V \rightarrow \gamma S}(s) &= \sqrt{s(s - 4m^2)} - 2m^2 \ln \frac{\sqrt{s} + \sqrt{s - 4m^2}}{\sqrt{s} - \sqrt{s - 4m^2}}. \end{aligned} \quad (38)$$

The total form factor is equal to

$$F_{V \rightarrow \gamma S} = F_{V(0) \rightarrow \gamma S} + F_{V(2) \rightarrow \gamma S}. \quad (39)$$

The charge factor of the transition  $V \rightarrow \gamma S$  for heavy quarks coincides with that for  $V \rightarrow \gamma P$ :  $Z_{V \rightarrow \gamma S} = Z_{V \rightarrow \gamma P}$ , see Eq. (30). Normalization condition for  $\psi_S(s)$  reads:

$$1 = \int_{4m^2}^{\infty} \frac{ds}{16\pi^2} \psi_S^2(s) 2m^2 (s - 4m^2) \sqrt{\frac{s - 4m^2}{s}}. \quad (40)$$

Working with the transition amplitude  $V \rightarrow \gamma S$ , one faces the ambiguity in writing the spin operator that is due to the existence of the nilpotent spin operator component — this problem is discussed in detail in [34, 35].

### 2.2.3 Transitions of the tensor ( $2^{++}$ ) and vector ( $1^{--}$ ) mesons

Three independent spin operators determine the transition amplitude  $T \rightarrow \gamma V$  and, correspondingly, we have three form factors [33]. In terms of the form factors  $F_{T \rightarrow \gamma V}^{(i)}$  ( $i = 1, 2, 3$ ), the partial widths for the decays  $T \rightarrow \gamma V$  and  $V \rightarrow \gamma T$  read:

$$\begin{aligned} m_T \Gamma_{T \rightarrow \gamma V} &= \frac{\alpha}{20} \frac{m_T^2 - m_V^2}{m_T^2} \left[ z_{11}^{\perp} (F_{T \rightarrow \gamma V}^{(1)})^2 + z_{22}^{\perp} (F_{T \rightarrow \gamma V}^{(2)})^2 + z_{33}^{\perp} (F_{T \rightarrow \gamma V}^{(3)})^2 \right], \\ m_V \Gamma_{V \rightarrow \gamma T} &= \frac{\alpha}{12} \frac{m_V^2 - m_T^2}{m_V^2} \left[ z_{11}^{\perp} (F_{T \rightarrow \gamma V}^{(1)})^2 + z_{22}^{\perp} (F_{T \rightarrow \gamma V}^{(2)})^2 + z_{33}^{\perp} (F_{T \rightarrow \gamma V}^{(3)})^2 \right]. \end{aligned} \quad (41)$$

Here,

$$\begin{aligned}
z_{11}^\perp &= \frac{3M_T^4 + 34M_T^2M_V^2 + 3M_V^4}{12M_T^2M_V^2}, \\
z_{22}^\perp &= 9 \frac{M_T^4 + 10M_T^2M_V^2 + M_V^4}{3M_T^4 + 34M_T^2M_V^2 + 3M_V^4}, \\
z_{33}^\perp &= \frac{9}{2} \frac{(M_T^2 + M_V^2)^2}{M_T^4 + 10M_T^2M_V^2 + M_V^4}.
\end{aligned} \tag{42}$$

The quark–antiquark  $2^{++}$  state is determined by two components of the wave function with the dominant  $P$ - and  $F$ -waves:

$$\psi_n^{(1,1,2)}(k^2) \equiv \psi_{T(1)}(s), \quad \psi_n^{(1,3,2)}(k^2) \equiv \psi_{T(3)}(s). \tag{43}$$

With these notations, the form factors  $F_{T(L) \rightarrow \gamma V(L')}^{(i)}$  for  $i = 1, 2, 3$  read:

$$F_{T(L) \rightarrow \gamma V(L')}^{(i)} = Z_{T(L) \rightarrow \gamma V(L')} \int_{4m^2}^{\infty} \frac{ds}{16\pi^2} S_{T(L) \rightarrow \gamma V(L')}^{(i)}(s) \psi_T(s) \psi_V(s). \tag{44}$$

Here,

$$\begin{aligned}
S_{T(1) \rightarrow \gamma V(0)}^{(1)}(s) &= -\frac{\sqrt{3}}{5}(8m^2 + 3s)I_{T \rightarrow \gamma V}^{(1)}(s), \\
S_{T(1) \rightarrow \gamma V(0)}^{(2)}(s) &= \frac{2}{3}S_{T(1) \rightarrow \gamma V(0)}^{(3)}(s) = -\frac{2}{3\sqrt{3}}I_{T \rightarrow \gamma V}^{(2)}(s), \\
S_{T(1) \rightarrow \gamma V(2)}^{(1)}(s) &= -\frac{\sqrt{6}}{40}(16m^2 - 3s)(4m^2 - s)I_{T \rightarrow \gamma V}^{(1)}(s), \\
S_{T(1) \rightarrow \gamma V(2)}^{(2)}(s) &= \frac{2}{3}S_{T(1) \rightarrow \gamma V(2)}^{(3)}(s) = -\frac{\sqrt{2}}{12\sqrt{3}}(8m^2 + s)I_{T \rightarrow \gamma V}^{(2)}(s), \\
S_{T(3) \rightarrow \gamma V(0)}^{(1)}(s) &= -\frac{3\sqrt{2}}{20}(4m^2 - s)^2I_{T \rightarrow \gamma V}^{(1)}(s), \\
S_{T(3) \rightarrow \gamma V(0)}^{(2)}(s) &= \frac{2}{3}S_{T(3) \rightarrow \gamma V(0)}^{(3)}(s) = -\frac{\sqrt{2}}{18}(6m^2 + s)I_{T \rightarrow \gamma V}^{(2)}(s), \\
S_{T(3) \rightarrow \gamma V(2)}^{(1)}(s) &= -\frac{3}{80}(4m^2 - s)^2(8m^2 + s)I_{T \rightarrow \gamma V}^{(1)}(s), \\
S_{T(3) \rightarrow \gamma V(2)}^{(2)}(s) &= \frac{2}{3}S_{T(3) \rightarrow \gamma V(2)}^{(3)}(s) = -\frac{1}{72}(16m^2 - 3s)(4m^2 - s)I_{T \rightarrow \gamma V}^{(2)}(s),
\end{aligned} \tag{45}$$

where

$$\begin{aligned}
I_{T \rightarrow \gamma V}^{(1)}(s) &= 2m^2 \ln \frac{\sqrt{s} + \sqrt{s - 4m^2}}{\sqrt{s} - \sqrt{s - 4m^2}} - \sqrt{s(s - 4m^2)}, \\
I_{T \rightarrow \gamma V}^{(2)}(s) &= m^2(m^2 + s) \ln \frac{\sqrt{s} + \sqrt{s - 4m^2}}{\sqrt{s} - \sqrt{s - 4m^2}} - \frac{1}{12} \sqrt{s(s - 4m^2)}(s + 26m^2).
\end{aligned} \tag{46}$$

The total form factor is a sum over four terms:

$$F_{T \rightarrow \gamma V}^{(i)} = \sum_{L, L'} F_{T^{(L)} \rightarrow \gamma V^{(L')}}^{(i)}. \quad (47)$$

Normalization condition for the tensor meson wave function is written in the  $s$ -integral representation as follows:

$$1 = W_{11}[T] + W_{13}[T] + W_{33}[T], \quad (48)$$

$$W_{11}[T] = \frac{1}{5} \int_{4m^2}^{\infty} \frac{ds}{16\pi^2} \psi_{T(1)}^2(s) \frac{1}{2} (8m^2 + 3s)(s - 4m^2) \sqrt{\frac{s - 4m^2}{s}}, \quad (49)$$

$$W_{13}[T] = \frac{1}{5} \int_{4m^2}^{\infty} \frac{ds}{16\pi^2} \psi_{T(1)}(s) \psi_{T(3)}(s) \frac{\sqrt{3}}{2\sqrt{2}} (s - 4m^2)^3 \sqrt{\frac{s - 4m^2}{s}},$$

$$W_{33}[T] = \frac{1}{5} \int_{4m^2}^{\infty} \frac{ds}{16\pi^2} \psi_{T(3)}^2(s) \frac{1}{16} (6m^2 + s)(s - 4m^2)^3 \sqrt{\frac{s - 4m^2}{s}}.$$

#### 2.2.4 Transitions of the pseudovector ( $1^{++}$ ) and vector ( $1^{--}$ ) mesons

Here we present the formulas for the radiative transitions of the vector ( $V$ ) and pseudovector ( $A$ ) mesons. The partial widths for the decays  $A \rightarrow \gamma V$  and  $V \rightarrow \gamma A$  are determined by the form factor  $F_{A \rightarrow \gamma V}$  as follows [33]:

$$\begin{aligned} m_A \Gamma_{A \rightarrow \gamma V} &= \frac{\alpha}{12} \frac{m_A^2 - m_V^2}{m_A^2} z_{AV}^\perp F_{A \rightarrow \gamma V}^2, \\ m_V \Gamma_{V \rightarrow \gamma A} &= \frac{\alpha}{12} \frac{m_V^2 - m_A^2}{m_V^2} z_{VA}^\perp F_{A \rightarrow \gamma V}^2, \end{aligned} \quad (50)$$

where

$$z_{AV}^\perp = -\frac{M_A^4 + 6M_A^2 M_V^2 + M_V^4}{2M_V^2}, \quad z_{VA}^\perp = -\frac{M_A^4 + 6M_A^2 M_V^2 + M_V^4}{2M_A^2}. \quad (51)$$

Changing notation

$$\psi_n^{(1,1,1)}(k^2) = \psi_A(s), \quad (52)$$

we write:

$$\begin{aligned} F_{A \rightarrow \gamma V(L)} &= Z_{A \rightarrow \gamma V(L)} \int_{4m^2}^{\infty} \frac{ds}{16\pi^2} S_{A \rightarrow \gamma V(L)}(s) \psi_A(s) \psi_{V(L)}(s), \\ S_{A \rightarrow \gamma V(0)}(s) &= -\sqrt{\frac{3}{2}} I_{A \rightarrow \gamma V}^{(1)}(s), \\ S_{A \rightarrow \gamma V(2)}(s) &= \frac{\sqrt{3}}{8} (4m^2 - s) I_{A \rightarrow \gamma V}^{(1)}(s), \end{aligned} \quad (53)$$

where

$$I_{A \rightarrow \gamma V}^{(1)}(s) = \sqrt{s} \left( 2m^2 \ln \frac{\sqrt{s} + \sqrt{s - 4m^2}}{\sqrt{s} - \sqrt{s - 4m^2}} - \sqrt{s(s - 4m^2)} \right). \quad (54)$$

The normalization condition reads:

$$1 = \frac{1}{2} \int_{4m^2}^{\infty} \frac{ds}{16\pi^2} \psi_A^2(s) s(s - 4m^2) \sqrt{\frac{s - 4m^2}{s}}. \quad (55)$$

### 2.3 Radiative transitions $e^+e^- \rightarrow V(Q\bar{Q})$ and $Q\bar{Q}$ -meson $\rightarrow \gamma\gamma$

For the consideration of the radiative transition processes  $e^+e^- \rightarrow V(Q\bar{Q})$  and  $\gamma\gamma \rightarrow Q\bar{Q}$ -meson, it is convenient to introduce the quark–antiquark components of the photon wave function [19, 22, 23]. The quark components of photon is tightly related to the determination of the quark wave functions of vector mesons.

The introduction of the quark–antiquark photon wave function may be illustrated by the two-photon meson decay. Dealing with the time-ordered processes, that is necessary in the dispersion relation or light-cone variable approaches, the  $Q\bar{Q}$ -meson  $\rightarrow \gamma\gamma$  decay should be treated as a two-step reaction: the emission of photon by the quark (Fig. 1a) or antiquark (Fig. 1b) and a subsequent annihilation  $Q\bar{Q} \rightarrow \gamma$ . The triangle diagram cuttings related to these two subprocesses are shown in Fig. 1c, thus leading to the representation of the triangle diagram in terms of the double dispersion integral. In the diagram 1c, on the left from the first cutting, there is the transition vertex of *quarkonium*  $\rightarrow Q\bar{Q}$ : we denote this vertex as  $G_{Q\bar{Q}}(s)$ . This vertex determines the wave function of the initial  $Q\bar{Q}$ -meson:

$$\frac{G_{Q\bar{Q}}(s)}{s - M^2} = \psi_{Q\bar{Q}}(s). \quad (56)$$

In the previous subsection, this wave function was denoted for different  $J^{PC}$  as  $\psi_V(s)$ ,  $\psi_P(s)$ ,  $\psi_S(s)$ , and so on.

Likewise, the right-hand cut in Fig. 1c describes the transition  $Q\bar{Q} \rightarrow \gamma$  and provides us with the factor

$$\frac{1}{s'} e_Q, \quad (57)$$

where  $s'$  is the invariant energy square of quarks in the final state and  $e_Q$  is the charge of the  $Q$ -quark. But when we deal with the transition  $Q\bar{Q} \rightarrow \gamma$ , the interaction of quarks should be necessarily taken into consideration.

The quarks may interact both in initial (Fig. 1d) and final (Fig. 1e) states. In fact, the interaction of quarks in the initial states has been accounted for in (56), because the vertex functions  $G_{Q\bar{Q}}$  (or wave functions  $\psi_P$ ,  $\psi_S$ , and so on) are the solutions of the spectral integral equation — this equation is shown diagrammatically in Fig. 1f. As concerns the quark interaction in the final state, it should be specially taken into account, in addition to the pointlike interaction (57). The diagram shown in Fig. 1g stands for the quark interaction in

the transition  $Q\bar{Q} \rightarrow \gamma$ , and we approximate it with the sum of pole terms of the vector meson ( $\Upsilon$ 's or  $\psi$ 's in the cases of  $b\bar{b}$  or  $c\bar{c}$  systems), see Fig. 1h. Accordingly, the factor related to the right-hand cut of Fig. 1c is written as follows:

$$\frac{G_{\gamma \rightarrow Q\bar{Q}}(s')}{s'} e_Q , \quad (58)$$

where the vertex function  $G_{\gamma \rightarrow Q\bar{Q}}(s')$  at  $s' \sim 4m_Q^2$  is the superposition of vertices of the  $V(n)$ -mesons (see Fig. 1h):

$$G_{\gamma \rightarrow Q\bar{Q}}(s) \simeq \sum_n C_n G_{V(n)}(s) , \quad s \sim 4m_Q^2 . \quad (59)$$

Here,  $n$  is the radial quantum number of  $V$ -meson and  $C_n$ 's are the coefficients which should be determined in the fit.

At large  $s$ , the vertex  $Q\bar{Q} \rightarrow \gamma$  is a pointlike one:

$$G_{\gamma \rightarrow Q\bar{Q}}(s) \simeq 1 \quad \text{at } s > s_0 . \quad (60)$$

The parameter  $s_0$  can be determined from the data on the  $e^+e^-$ -annihilation into hadrons: it defines the energy range where the ratio  $R(s) = \sigma(e^+e^- \rightarrow \text{hadrons})/\sigma(e^+e^- \rightarrow \mu^+\mu^-)$  reaches a constant-behavior regime above the threshold of the production of heavy mesons. The data [36] give us  $s_0 \sim (10 - 15) \text{ GeV}^2$  for the  $c\bar{c}$  component and  $s_0 \sim (100 - 150) \text{ GeV}^2$  for the  $b\bar{b}$  one.

Therefore, to describe the transition  $Q\bar{Q} \rightarrow \gamma$  we may introduce the characteristics which, similarly to (56), can be called the  $Q\bar{Q}$ -component of the photon wave function:

$$\frac{G_{\gamma \rightarrow Q\bar{Q}}(s)}{s - q^2} = \Psi_{\gamma(q^2) \rightarrow Q\bar{Q}}(s) . \quad (61)$$

Here  $q$  is the photon four-momentum. Let us emphasize that such a wave function is determined at  $s \gtrsim 4m_Q^2$ .

There are more reactions which are promptly determined by the photon wave function. These are the transitions  $e^+e^- \rightarrow \Upsilon$  and  $e^+e^- \rightarrow \psi$ , see Fig. 2: here the loop diagram is defined by the convolution of the vector meson wave function and  $G_{\gamma \rightarrow Q\bar{Q}}$ .

The transition  $\gamma \rightarrow Q\bar{Q}$  is determined by two spin structures,  $\gamma_\alpha$  and  $\frac{3}{2} [k_\alpha \hat{k} - \frac{1}{3} k^2 \gamma_\alpha^\perp]$  (see Eq.(23)) and, correspondingly, by two vertices.

$$\gamma_\alpha G_{\gamma \rightarrow Q\bar{Q}}^{(S)}(s) , \quad \gamma_\xi X_{\xi\alpha}^{(2)} G_{\gamma \rightarrow Q\bar{Q}}^{(D)}(s) \quad (62)$$

It means that we take into account the normal quark-photon interaction,  $\gamma_\alpha$ , as well as the contribution of the anomalous magnetic moment.

For the vertex function of the transition  $\gamma \rightarrow Q\bar{Q}$  we use the following fitting formula:

$$G_{\gamma \rightarrow Q\bar{Q}}^{(S)}(s) = \sum_{n=1}^6 C_{nS} G_{V(nS)}(s) + \frac{1}{1 + \exp(-\beta_\gamma(s - s_0))} , \quad (63)$$

$$G_{\gamma \rightarrow Q\bar{Q}}^{(D)}(s) = \sum_{n=1}^6 C_{nD} G_{V(nD)}(s) ,$$

where  $G_{V(nS)}(s) = \psi_n^{(101)}(s)(s - M_{V(nS)}^2)$  and  $G_{V(nD)}(s) = \psi_n^{(121)}(s)(s - M_{V(nD)}^2)$ . The parameters  $C_{nS}$ ,  $C_{nD}$ ,  $\beta_\gamma$  and  $s_0$  are determined in the fit.

### 2.3.1 Decay $V \rightarrow e^+e^-$

The transition amplitudes  $V \rightarrow e^+e^-$  were calculated in [23, 37]. The partial width for the decay  $V \rightarrow e^+e^-$  reads:

$$\Gamma(V \rightarrow e^+e^-) = \frac{\pi\alpha^2}{M_V^5} \sqrt{\frac{M_V^2 - 4\mu_e^2}{M_V^2}} \left( \frac{8}{3}\mu_e^2 + \frac{4}{3}M_V^2 \right) |F_{V \rightarrow e^+e^-}|^2, \quad (64)$$

where  $\mu_e$  is the electron mass,  $M_V$  is the measured vector quarkonium mass, and the form factor  $F_{V \rightarrow e^+e^-}$  is determined by the process of Fig. 2. The quark loops in Fig. 2 are different for the  $S$ - and  $D$ -wave  $Q\bar{Q}$  states, so we have two transition amplitudes  $F_{V(n,L) \rightarrow e^+e^-}$ , with  $L = 0$  and  $L = 2$ :

$$F_{V \rightarrow e^+e^-} = F_{V(0) \rightarrow e^+e^-} + F_{V(2) \rightarrow e^+e^-}, \quad (65)$$

where

$$F_{V(0) \rightarrow e^+e^-} = Z_{Q\bar{Q}}^{V \rightarrow e^+e^-} \sqrt{N_c} \int_{4m^2}^{\infty} \frac{ds}{16\pi^2} \psi_{V(0)}(s) G_{\gamma \rightarrow Q\bar{Q}}^{(S)}(s) \left( \frac{8}{3}m^2 + \frac{4}{3}s \right) \sqrt{\frac{s - 4m^2}{s}}, \quad (66)$$

$$F_{V(2) \rightarrow e^+e^-} = Z_{Q\bar{Q}}^{V \rightarrow e^+e^-} \sqrt{N_c} \int_{4m^2}^{\infty} \frac{ds}{16\pi^2} \psi_{V(2)}(s) G_{\gamma \rightarrow Q\bar{Q}}^{(D)}(s) \frac{(s - 4m^2)^2}{6} \sqrt{\frac{s - 4m^2}{s}}.$$

At  $L = 0, 2$ , the wave functions  $\psi_{V(L)}(s)$  are normalized according to (33); here the charge factors are  $Z_{bb}^{V \rightarrow e^+e^-} = -1/3$  and  $Z_{cc}^{V \rightarrow e^+e^-} = 2/3$ .

### 2.3.2 Decay $P \rightarrow \gamma\gamma$

The two-photon decays of pseudoscalar  $q\bar{q}$  mesons ( $L = 0$ ) were studied in [19, 22]. Partial width for the decay  $P \rightarrow \gamma\gamma$  reads:

$$\Gamma(P \rightarrow \gamma\gamma) = \frac{\pi}{4} \alpha^2 M_P^3 |F_{P \rightarrow \gamma\gamma}|^2. \quad (67)$$

The transition amplitude is determined by the processes of Figs. 1a, b, it reads:

$$F_{P \rightarrow \gamma\gamma} = Z_{Q\bar{Q}}^{\gamma\gamma} \sqrt{N_c} m \int_{4m^2}^{\infty} \frac{ds}{2\pi^2} \psi_P(s) \Psi_{\gamma \rightarrow Q\bar{Q}}(s) \ln \frac{\sqrt{s} + \sqrt{s - 4m^2}}{\sqrt{s} - \sqrt{s - 4m^2}}. \quad (68)$$

Recall that  $\Psi_{\gamma \rightarrow Q\bar{Q}}(s) = G_{\gamma \rightarrow Q\bar{Q}}(s)/s$ . To underline the existence of decays with different radial excited states, we introduce the index  $n$  in (68). Normalization of  $\psi_P(s)$  is given by (35), and

$$Z_{bb}^{\gamma\gamma} = \frac{2}{9}, \quad Z_{cc}^{\gamma\gamma} = \frac{8}{9}. \quad (69)$$

### 2.3.3 Decay $S \rightarrow \gamma\gamma$

The two-photon decay of the  $0^{++}q\bar{q}$  mesons ( $L = 1$ ) was considered in [19, 20]. The partial width of the decay  $S(n) \rightarrow \gamma\gamma$  ( $n$  is radial quantum number) reads:

$$\Gamma(S \rightarrow \gamma\gamma) = \frac{\pi\alpha^2}{M_S} |F_{S(n) \rightarrow \gamma\gamma}|^2, \quad (70)$$

with the quark transition amplitude (Figs. 1a,b) equal to:

$$F_{S(n) \rightarrow \gamma\gamma} = Z_{Q\bar{Q}}^{\gamma\gamma} \sqrt{N_c} m^2 \int_{4m^2}^{\infty} \frac{ds}{4\pi^2} \psi_{S(n)}(s) \Psi_{\gamma \rightarrow Q\bar{Q}}(s) \times \left( \sqrt{s(s-4m^2)} - 2m^2 \ln \frac{\sqrt{s} + \sqrt{s-4m^2}}{\sqrt{s} - \sqrt{s-4m^2}} \right). \quad (71)$$

Normalization of  $\psi_{S(n)}(s)$  is given by (40).

### 2.3.4 Decay $T \rightarrow \gamma\gamma$

The two-photon tensor meson decay amplitude was calculated in [19, 21]. The partial width for the decay process  $T \rightarrow \gamma\gamma$  is defined by two transition amplitudes with the helicities  $H = 0, 2$ :

$$\Gamma(T \rightarrow \gamma\gamma) = \frac{4}{5} \frac{\pi\alpha^2}{M_T} \left[ \frac{1}{6} |F_{T \rightarrow \gamma\gamma}^{(0)}|^2 + |F_{T \rightarrow \gamma\gamma}^{(2)}|^2 \right]. \quad (72)$$

Taking into account the  $P$ - and  $F$ -wave quark–antiquark component, we write the form factors  $F_{T \rightarrow \gamma\gamma}^{(H)}$  as

$$F_{T \rightarrow \gamma\gamma}^{(H)} = F_{T(1) \rightarrow \gamma\gamma}^{(H)} + F_{T(3) \rightarrow \gamma\gamma}^{(H)}, \quad (73)$$

where

$$F_{T(L) \rightarrow \gamma\gamma}^{(H)} = Z_{Q\bar{Q}}^{\gamma\gamma} \sqrt{N_c} \int_{4m^2}^{\infty} \frac{ds}{16\pi^2} \psi_{T(L)}(s) \Psi_{\gamma \rightarrow Q\bar{Q}}(s) S_{T(L) \rightarrow \gamma\gamma}^{(H)}(s), \quad (74)$$

with the following spin factors:

$$\begin{aligned} S_{T(1) \rightarrow \gamma\gamma}^{(0)}(s) &= -\frac{4}{\sqrt{3}} \sqrt{s(s-4m^2)} (12m^2 + s) + \frac{8m^2}{\sqrt{3}} (4m^2 + 3s) \ln \frac{s + \sqrt{s(s-4m^2)}}{s - \sqrt{s(s-4m^2)}}, \\ S_{T(3) \rightarrow \gamma\gamma}^{(0)}(s) &= -\frac{2\sqrt{2s(s-4m^2)}}{5} (72m^4 + 8m^2s + s^2) + \\ &+ \frac{12\sqrt{2}}{5} m^2 (8m^4 + 4m^2s + s^2) \ln \frac{s + \sqrt{s(s-4m^2)}}{s - \sqrt{s(s-4m^2)}}, \end{aligned} \quad (75)$$



and

$$\begin{aligned}
S_{T(1) \rightarrow \gamma\gamma}^{(2)}(s) &= \frac{8\sqrt{s(s-4m^2)}}{3\sqrt{3}} (5m^2 + s) - \frac{8m^2}{\sqrt{3}} (2m^2 + s) \ln \frac{s + \sqrt{s(s-4m^2)}}{s - \sqrt{s(s-4m^2)}}, \\
S_{T(3) \rightarrow \gamma\gamma}^{(2)}(s) &= \frac{2\sqrt{2s(s-4m^2)}}{15} (30m^4 - 4m^2s + s^2) - \\
&\quad - \frac{2\sqrt{2}}{5} m^2 (12m^4 - 2m^2s + s^2) \ln \frac{s + \sqrt{s(s-4m^2)}}{s - \sqrt{s(s-4m^2)}}.
\end{aligned} \tag{76}$$

Normalization of  $\psi_{T(1)}(s)$  and  $\psi_{T(3)}(s)$  is determined by (48).

### 3 Bottomonium states found from spectral integral equation and radiative transitions

The quarkonium wave functions are fitted in the following form:

$$\psi_{(n)}^{(S,L,J)}(k^2) = e^{-\beta k^2} \sum_{i=1}^9 c_i(S, L, J; n) k^{i-1}, \tag{77}$$

where we re-denoted  $k^2 \equiv \mathbf{k}^2$ ; recall that  $s = 4m^2 + 4\mathbf{k}^2$ . The fitting parameter  $\beta$  is of the order of  $0.5 - 1.5 \text{ GeV}^{-2}$  and may be different for different flavor sectors. We put here  $\beta = 1.2 \text{ GeV}^{-2}$

The data in the  $b\bar{b}$  sector can be described by two types of the  $t$ -channel exchanges, scalar and vector ones:  $\text{I} \otimes \text{I}$ ,  $\gamma_\mu \otimes \gamma_\mu$ . The addition of the pseudoscalar exchanges like  $\gamma_5 \otimes \gamma_5$  does not improve the fit.

Here, we present three variants of fit: with instantaneous forces (solution  $I(b\bar{b})$ ), retarded interactions (solution  $R(b\bar{b})$ ) and that with the universal "confinement potential" – instantaneous interaction with nearly the same parameters  $a$  and  $b$  in (21) for all the quark sectors:  $b\bar{b}$ ,  $c\bar{c}$  and  $q\bar{q}$  (solution  $U(b\bar{b})$ ).

For the  $b\bar{b}$  sector, the parameters for scalar and vector exchange interactions ( $\text{I} \otimes \text{I}$  and  $\gamma_\mu \otimes \gamma_\mu$ , see Section 2.2) are as follows (all values are in GeV):

Interaction	Wave	$a$	$b$	$c$	$\mu_c$	$d$	$\mu_d$
$(\text{I} \otimes \text{I})$	$I(b\bar{b})$	-0.151	0.160	0.506	0.201	-0.250	0.201
	$U(b\bar{b})$	0.911	0.150	-0.377	0.401	-0.201	0.401
	$R(b\bar{b})$	-0.680	0.130	1.322	0.201	-0.228	0.401
$(\gamma_\mu \otimes \gamma_\mu)$	$I(b\bar{b})$	-0.812	0.000	0.867	0.401	0.300	0.001
	$U(b\bar{b})$	1.178	-0.150	-1.356	0.201	0.500	0.001
	$R(b\bar{b})$	-1.620	-0.005	1.821	0.201	0.311	0.001

### 3.1 Masses of the $b\bar{b}$ states

The fitting procedure prefers for the constituent  $b$ -quark the mass value  $m_b = 4.5$  GeV. This value looks quite reasonable if we take into account that mass difference of the constituent and QCD quarks is of the order of 200 – 350 MeV and the QCD estimates [38] give the constraint  $4.0 \leq m_b(QCD) \leq 4.5$  GeV.

The masses of  $b\bar{b}$  states for  $n = 1, 2, 3, 4, 5, 6$  (experimental values and those obtained in the fit) are given below, in (79) – (84). The bold numbers stand for the masses, which are included in the fitting procedure. In parentheses we show the dominant wave for  $b\bar{b}$  state ( $S$  or  $D$  for  $1^{--}$  and  $P$  or  $F$  for  $2^{++}$ ). The right-hand side columns show the mean square radii of bottomonia (in  $\text{GeV}^{-2}$  for solution  $I(b\bar{b})$ ).

We have the following masses (in GeV) for  $1^{--}$  states:

State	Data	$I(b\bar{b})$	$U(b\bar{b})$	$R(b\bar{b})$	$R_I^2$
$\Upsilon(1S)$	<b>9.460</b>	9.392 ( $S$ )	9.382 ( $S$ )	9.448 ( $S$ )	0.342
$\Upsilon(2S)$	<b>10.023</b>	10.029 ( $S$ )	10.027 ( $S$ )	10.023 ( $S$ )	1.632
$\Upsilon(1D)$	10.150	10.159 ( $D$ )	10.158 ( $D$ )	10.105 ( $D$ )	0.342
$\Upsilon(3S)$	<b>10.355</b>	10.368 ( $S$ )	10.365 ( $S$ )	10.362 ( $S$ )	3.794
$\Upsilon(2D)$	10.450	10.439 ( $D$ )	10.436 ( $D$ )	10.156 ( $D$ )	1.632
$\Upsilon(4S)$	<b>10.580</b>	10.615 ( $S$ )	10.634 ( $S$ )	10.628 ( $S$ )	6.504
$\Upsilon(3D)$	10.700	10.661 ( $D$ )	10.677 ( $D$ )	10.430 ( $D$ )	3.794
$\Upsilon(5S)$	<b>10.865</b>	10.819 ( $S$ )	10.872 ( $S$ )	10.851 ( $S$ )	9.793
$\Upsilon(4D)$	10.950	10.852 ( $D$ )	10.898 ( $D$ )	10.669 ( $D$ )	6.504
$\Upsilon(6S)$	<b>11.020</b>	11.019 ( $S$ )	11.084 ( $S$ )	11.040 ( $S$ )	11.990
$\Upsilon(5D)$	—	11.023 ( $D$ )	11.109 ( $D$ )	10.892 ( $D$ )	9.793
$\Upsilon(6D)$	—	11.214 ( $D$ )	11.303 ( $D$ )	11.085 ( $D$ )	11.990 ,

for  $0^{-+}$  states:

State	Data	$I(b\bar{b})$	$U(b\bar{b})$	$R(b\bar{b})$	$R_I^2$
$\eta_b(1S)$	<b>9.300</b>	9.334	9.322	9.393	0.922
$\eta_b(2S)$	—	10.006	10.011	10.007	2.782
$\eta_b(3S)$	—	10.344	10.355	10.352	5.781
$\eta_b(4S)$	—	10.557	10.626	10.621	18.839
$\eta_b(5S)$	—	10.636	10.864	10.846	13.699
$\eta_b(6S)$	—	10.837	11.079	11.037	11.668 ,

for  $0^{++}$  states:

State	Data	$I(b\bar{b})$	$U(b\bar{b})$	$R(b\bar{b})$	$R_I^2$
$\chi_{b0}(1P)$	<b>9.859</b>	9.852	9.862	9.851	0.847
$\chi_{b0}(2P)$	<b>10.232</b>	10.241	10.236	10.227	2.632
$\chi_{b0}(3P)$	—	10.509	10.517	10.510	5.161
$\chi_{b0}(4P)$	—	10.726	10.759	10.745	8.053
$\chi_{b0}(5P)$	—	10.884	10.983	10.952	12.437
$\chi_{b0}(6P)$	—	10.947	11.185	11.084	19.969 ,

for  $1^{++}$  states:

State	Data	$I(b\bar{b})$	$U(b\bar{b})$	$R(b\bar{b})$	$R_I^2$
$\chi_{b1}(1P)$	<b>9.892</b>	9.884	9.895	9.890	0.915
$\chi_{b1}(2P)$	<b>10.255</b>	10.257	10.252	10.249	2.777
$\chi_{b1}(3P)$	—	10.516	10.528	10.526	5.814
$\chi_{b1}(4P)$	—	10.697	10.767	10.762	18.944
$\chi_{b1}(5P)$	—	10.759	10.989	10.970	13.544
$\chi_{b1}(6P)$	—	10.920	11.191	11.199	11.702 ,

for  $2^{++}$  states:

State	Data	$I(b\bar{b})$	$U(b\bar{b})$	$R(b\bar{b})$	$R_I^2$
$\chi_{b2}(1P)$	<b>9.912</b>	9.909 ( $P$ )	9.911 ( $P$ )	9.923 ( $P$ )	0.956
$\chi_{b2}(2P)$	<b>10.268</b>	10.270 ( $P$ )	10.262 ( $P$ )	10.268 ( $P$ )	2.782
$\chi_{b2}(1F)$	—	10.365 ( $F$ )	10.347 ( $F$ )	10.346 ( $F$ )	0.956
$\chi_{b2}(3P)$	—	10.528 ( $P$ )	10.535 ( $P$ )	10.538 ( $P$ )	5.361
$\chi_{b2}(2F)$	—	10.594 ( $F$ )	10.592 ( $F$ )	10.592 ( $F$ )	2.782
$\chi_{b2}(4P)$	—	10.738 ( $P$ )	10.773 ( $P$ )	10.768 ( $P$ )	8.573
$\chi_{b2}(3F)$	—	10.788 ( $P$ )	10.813 ( $F$ )	10.807 ( $F$ )	5.361
$\chi_{b2}(5F)$	—	10.846 ( $F$ )	10.994 ( $P$ )	10.972 ( $P$ )	18.995
$\chi_{b2}(4F)$	—	10.963 ( $P$ )	11.020 ( $F$ )	11.006 ( $F$ )	8.573
$\chi_{b2}(6F)$	—	10.931 ( $F$ )	11.196 ( $P$ )	11.150 ( $P$ )	13.978
$\chi_{b2}(5F)$	—	11.124 ( $F$ )	11.221 ( $F$ )	11.187 ( $F$ )	18.995
$\chi_{b2}(6F)$	—	11.326 ( $F$ )	11.411 ( $F$ )	11.380 ( $F$ )	13.978 ,

and for  $1^{+-}$  states,  $h_b(1^{+-})$ :

State	Data	$I(b\bar{b})$	$U(b\bar{b})$	$R(b\bar{b})$	$R_I^2$
$h_b(1S)$	—	9.889	9.902	9.896	0.922
$h_b(2S)$	—	10.259	10.255	10.253	2.782
$h_b(3S)$	—	10.518	10.530	10.529	5.781
$h_b(4S)$	—	10.700	10.768	10.764	18.839
$h_b(5S)$	—	10.759	10.990	10.971	13.699
$h_b(6S)$	—	10.921	11.192	11.200	11.668 .

The wave functions for solution  $I(b\bar{b})$  are presented in Appendix II: we show the wave functions in the  $k$ -representation and give coefficients  $c_i$ ,  $\beta$  for Eq. (77). For  $1^{--}$  and  $2^{++}$  states, we give  $W_{LL'}$ : one can see that the admixture of second components is small.

### 3.2 Radiative decays $(b\bar{b})_{in} \rightarrow \gamma(b\bar{b})_{out}$

Figure 3 shows the radiative transitions which are included into the fitting procedure.

The fit gives us the following values for radiative decay of  $\Upsilon$ -mesons (partial widths in keV):

Process	Data	$I(b\bar{b})$	$U(b\bar{b})$	$R(b\bar{b})$	[7]	[8]
$\Upsilon(1S) \rightarrow \gamma\eta_{b0}(1S)$	—	0.0092	0.0100	0.0079	—	—
$\Upsilon(2S) \rightarrow \gamma\eta_{b0}(1S)$	—	0.0025	0.0015	0.0008	—	—
$\Upsilon(2S) \rightarrow \gamma\eta_{b0}(2S)$	—	0.0006	0.0002	0.0002	—	—
$\Upsilon(2S) \rightarrow \gamma\chi_{b0}(1P)$	$1.7 \pm 0.2$	1.1023	1.0669	0.9611	1.62	1.41
$\Upsilon(2S) \rightarrow \gamma\chi_{b1}(1P)$	$3.0 \pm 0.5$	2.7288	2.3675	2.1268	2.55	2.27
$\Upsilon(2S) \rightarrow \gamma\chi_{b2}(1P)$	$3.1 \pm 0.5$	2.9100	2.6674	1.9367	2.51	2.24
$\Upsilon(3S) \rightarrow \gamma\eta_{b0}(1S)$	—	0.0016	0.0007	0.0005	—	—
$\Upsilon(3S) \rightarrow \gamma\eta_{b0}(2S)$	—	0.0013	0.0000	0.0002	—	—
$\Upsilon(3S) \rightarrow \gamma\eta_{b0}(3S)$	—	0.0006	0.0001	0.0001	—	—
$\Upsilon(3S) \rightarrow \gamma\chi_{b0}(2P)$	$1.4 \pm 0.2$	1.1191	1.3746	1.1253	1.77	—
$\Upsilon(3S) \rightarrow \gamma\chi_{b1}(2P)$	$3.0 \pm 0.5$	3.4368	4.0831	3.1279	2.88	—
$\Upsilon(3S) \rightarrow \gamma\chi_{b2}(2P)$	$3.0 \pm 0.5$	3.7266	4.7438	3.1686	3.14	—

(85)

For the illustration, in (85) we present the results of Refs. [7, 8].

The radiative decay of  $\chi_{bJ}$  is not included into fitting procedure. We have the following predictions for the partial widths (in keV):

Process	Data	$I(b\bar{b})$	$U(b\bar{b})$	$R(b\bar{b})$
$\chi_{b0}(1P) \rightarrow \gamma\Upsilon(1S)$	$< \Gamma_{tot}(\chi_{b0}(1P)) \cdot 6 \cdot 10^{-2}$	43.49	52.79	34.47
$\chi_{b1}(1P) \rightarrow \gamma\Upsilon(1S)$	$\Gamma_{tot}(\chi_{b1}(1P)) \cdot (35 \pm 8) \cdot 10^{-2}$	53.31	63.77	42.62
$\chi_{b2}(1P) \rightarrow \gamma\Upsilon(1S)$	$\Gamma_{tot}(\chi_{b2}(1P)) \cdot (22 \pm 4) \cdot 10^{-2}$	47.61	56.15	38.10
$\chi_{b0}(2P) \rightarrow \gamma\Upsilon(1S)$	$\Gamma_{tot}(\chi_{b0}(2P)) \cdot (0.9 \pm 0.6) \cdot 10^{-2}$	7.49	9.25	7.08
$\chi_{b0}(2P) \rightarrow \gamma\Upsilon(2S)$	$\Gamma_{tot}(\chi_{b0}(2P)) \cdot (4.6 \pm 2.1) \cdot 10^{-2}$	11.94	15.88	11.06
$\chi_{b1}(2P) \rightarrow \gamma\Upsilon(1S)$	$\Gamma_{tot}(\chi_{b1}(2P)) \cdot (8.5 \pm 1.3) \cdot 10^{-2}$	12.76	16.85	11.69
$\chi_{b1}(2P) \rightarrow \gamma\Upsilon(2S)$	$\Gamma_{tot}(\chi_{b1}(2P)) \cdot (21.0 \pm 4.0) \cdot 10^{-2}$	12.92	14.40	16.01
$\chi_{b2}(2P) \rightarrow \gamma\Upsilon(1S)$	$\Gamma_{tot}(\chi_{b2}(2P)) \cdot (7.1 \pm 1.0) \cdot 10^{-2}$	18.11	20.58	12.37
$\chi_{b2}(2P) \rightarrow \gamma\Upsilon(2S)$	$\Gamma_{tot}(\chi_{b2}(2P)) \cdot (16.2 \pm 2.4) \cdot 10^{-2}$	16.14	18.25	14.41
$\chi_{b0}(3P) \rightarrow \gamma\Upsilon(1S)$	—	2.69	3.56	2.84
$\chi_{b1}(3P) \rightarrow \gamma\Upsilon(1S)$	—	4.41	7.06	5.43
$\chi_{b2}(3P) \rightarrow \gamma\Upsilon(1S)$	—	5.60	8.11	6.01
$\chi_{b0}(3P) \rightarrow \gamma\Upsilon(2S)$	—	2.05	1.86	2.04
$\chi_{b1}(3P) \rightarrow \gamma\Upsilon(2S)$	—	3.38	3.88	4.09
$\chi_{b2}(3P) \rightarrow \gamma\Upsilon(2S)$	—	4.37	4.59	4.57
$\chi_{b0}(3P) \rightarrow \gamma\Upsilon(3S)$	—	7.59	10.37	7.19
$\chi_{b1}(3P) \rightarrow \gamma\Upsilon(3S)$	—	10.74	15.85	11.33
$\chi_{b2}(3P) \rightarrow \gamma\Upsilon(3S)$	—	9.90	13.81	9.87

(86)

The total widths  $\Gamma_{tot}(\chi_{bJ}(1P))$  and  $\Gamma_{tot}(\chi_{bJ}(2P))$ , with  $J = 0, 1, 2$ , have not been measured yet.

The calculations performed on the basis of (86) give us the following estimates for total widths:

$$\Gamma_{tot}(\chi_{b0}(1P)) < 730 \text{ keV}, \quad (87)$$

$$\begin{aligned}
\Gamma_{tot}(\chi_{b1}(1P)) &\simeq 120 - 200 \text{ keV}, \\
\Gamma_{tot}(\chi_{b2}(1P)) &\simeq 180 - 270 \text{ keV}, \\
\Gamma_{tot}(\chi_{b0}(2P)) &\simeq 180 - 480 \text{ keV}, \\
\Gamma_{tot}(\chi_{b1}(2P)) &\simeq 50 - 80 \text{ keV}, \\
\Gamma_{tot}(\chi_{b2}(2P)) &\simeq 70 - 120 \text{ keV}.
\end{aligned}$$

The fit gives us the following values for partial widths of radiative decays of  $\eta_{b0}$ -mesons:

Process	Data	$I(b\bar{b})$	$U(b\bar{b})$	$R(b\bar{b})$	
$\eta_{b0}(2S) \rightarrow \gamma\Upsilon(1S)$	—	0.21	0.20	0.12	(88)
$\eta_{b0}(3S) \rightarrow \gamma\Upsilon(1S)$	—	0.27	0.18	0.11	
$\eta_{b0}(3S) \rightarrow \gamma\Upsilon(2S)$	—	0.05	0.02	0.01	

### 3.3 The $b\bar{b}$ component of the photon wave function

Fitting to the reactions with the  $\gamma \rightarrow b\bar{b}$  transitions, we determined the parameters  $C_n, \beta_\gamma, s_0$  defined in (63) for  $G_{\gamma \rightarrow b\bar{b}}^{S,D}(s)$ . For solutions  $R(b\bar{b}), I(b\bar{b})$  and  $U(b\bar{b})$ , they are as follows (in GeV):

$I(b\bar{b})$	$U(b\bar{b})$	$R(b\bar{b})$	
$C_{1S} = -0.263$	$C_{1S} = -0.800$	$C_{1S} = -0.220$	(89)
$C_{2S} = -0.296$	$C_{2S} = -0.303$	$C_{2S} = 0.092$	
$C_{3S} = 0.057$	$C_{3S} = 0.074$	$C_{3S} = -0.038$	
$C_{4S} = 0.298$	$C_{4S} = 0.197$	$C_{4S} = -0.027$	
$C_{5S} = -2.000$	$C_{5S} = -0.781$	$C_{5S} = 0.262$	
$C_{6S} = 1.093$	$C_{6S} = 2.000$	$C_{6S} = -0.441$	
$C_{1D} = -0.554$	$C_{1D} = -0.328$	$C_{1D} = 0.168$	
$C_{2D} = -0.284$	$C_{2D} = 0.233$	$C_{2D} = 0.109$	
$b_\gamma = 2.85$	$b_\gamma = 2.85$	$b_\gamma = 2.85$	
$s_0 = 18.79$	$s_0 = 18.79$	$s_0 = 18.79$	

Experimental values of partial widths included into fitting procedure as an input together with those obtained in the fitting procedure are shown below:

Process	Data	$I(b\bar{b})$	$U(b\bar{b})$	$R(b\bar{b})$	[39]	
$\Upsilon(1S) \rightarrow e^+e^-$	$1.314 \pm 0.029$	1.314	1.313	1.314	1.01	(90)
$\Upsilon(2S) \rightarrow e^+e^-$	$0.576 \pm 0.024$	0.576	0.575	0.576	0.35	
$\Upsilon(3S) \rightarrow e^+e^-$	$0.476 \pm 0.076$	0.476	0.476	0.476	0.25	
$\Upsilon(4S) \rightarrow e^+e^-$	$0.248 \pm 0.031$	0.248	0.248	0.248	0.22	
$\Upsilon(5S) \rightarrow e^+e^-$	$0.31 \pm 0.07$	0.310	0.310	0.310	0.18	
$\Upsilon(6S) \rightarrow e^+e^-$	$0.130 \pm 0.03$	0.130	0.130	0.130	0.14	

The last column in (90) demonstrates the results of [39].

The vertices  $G_{\gamma \rightarrow b\bar{b}}(s)$ , which represent our solutions and given in (89), are shown shown in Fig 4. The data and predictions for the two-photon partial widths  $\eta_{b0} \rightarrow \gamma\gamma, \chi_{b0} \rightarrow \gamma\gamma$ ,

$\chi_{b2} \rightarrow \gamma\gamma$  are as follows:

Process	Data	$I(b\bar{b})$	$U(b\bar{b})$	$R(b\bar{b})$	[40]	[41]	[42]	[43]	[44]	[45]
$\eta_{b0}(1S) \rightarrow \gamma\gamma$	—	1.554	1.851	1.537	0.35	0.22	0.46	0.46	0.45	0.17
$\eta_{b0}(2S) \rightarrow \gamma\gamma$	—	1.928	2.296	1.906	0.11	—	0.20	0.21	0.13	—
$\eta_{b0}(3S) \rightarrow \gamma\gamma$	—	2.139	2.547	2.115	0.10	0.084	—	—	—	—
$\chi_{b0}(1P) \rightarrow \gamma\gamma$	—	0.024	0.029	0.021	0.038	0.024	0.080	0.043	—	—
$\chi_{b0}(2P) \rightarrow \gamma\gamma$	—	0.023	0.028	0.021	0.029	0.026	—	—	—	—
$\chi_{b0}(3P) \rightarrow \gamma\gamma$	—	0.023	0.027	0.020	—	—	—	—	—	—
$\chi_{b2}(1P) \rightarrow \gamma\gamma$	—	0.016	0.020	0.013	0.0080	0.0056	0.0080	0.0074	—	—
$\chi_{b2}(2P) \rightarrow \gamma\gamma$	—	0.015	0.020	0.013	0.0060	0.0068	—	—	—	—
$\chi_{b2}(3P) \rightarrow \gamma\gamma$	—	0.015	0.019	0.012	—	—	—	—	—	—

(91)

The last six columns represent the calculation results of [40–45].

### 3.4 Potentials in the solution $I(b\bar{b})$

To be illustrative, let us demonstrate the interaction in one of the solutions, say,  $I(b\bar{b})$ , in the language of potentials.

In the solution  $I(b\bar{b})$ , the confinement potential is due to scalar exchanges only,  $V_{conf}^{(S)}(r) = -0.151 + 0.160r$  (GeV), it is shown in Fig. 5a. For the illustration, we demonstrate also the  $0^{-+}$ -levels created by this confinement potential alone. However, the scalar exchange has the short-range component  $V_{short}^{(S)}(r) = 0.506 \exp(-0.2r) - 0.250/r \exp(-0.2r)$  (GeV), see Fig. 5b, which pushes the levels higher. The potential related to the  $t$ -channel vector exchanges,  $V^{(V)}(r) = 0.812 - 0.867 \exp(-0.4r) - 0.300/r$  (GeV), does not contain the increasing part ( $\sim r$ ), see Fig. 5c. The last term may be interpreted as a one-gluon exchange, with  $\alpha_s = 0.300 \cdot 3/4 \simeq 0.23$ . Also in Fig. 5c, we demonstrate for the illustration the  $0^{-+}$ -levels, which would be created by vector exchange forces only.

In the solution  $U(b\bar{b})$ , the vector-exchange forces contain the one-gluon exchange term:  $V_{short}^{(V)}(r) = 1.355 \exp(-0.5r) - 0.500/r$  (GeV) which corresponds to  $\alpha_s \simeq 0.38$ .

## 4 Conclusion

In the framework of the method, which is in fact a variant of the dispersion relation approach, we have performed the description of the bottomonium spectra: the  $b\bar{b}$ -levels and their radiative transitions such as  $(b\bar{b})_{in} \rightarrow \gamma + (b\bar{b})_{out}$ ,  $e^+e^- \rightarrow V(b\bar{b})$  and  $b\bar{b}\text{-meson} \rightarrow \gamma\gamma$ . Using quark–antiquark interaction as an input, we have obtained several variants of a reasonably good fit of the data. The ambiguities in a reconstruction of the soft region  $b\bar{b}$  interaction underline the problem we face: a scarcity of the radiative decay data. To restore the  $b\bar{b}$  interaction, one needs much more data, in particular, on the two-photon reactions:  $\gamma\gamma \rightarrow b\bar{b}\text{-meson}$ , including the bottomonium production by virtual photons in  $\gamma\gamma^*$  and  $\gamma^*\gamma^*$  collisions.

We pay a considerable attention to the presentation of the  $b\bar{b}$  wave functions. The matter is that a solution may represent rather similarly the state levels, though with different wave functions. Therefore, we think that solution should be characterized by two characteristics, that is, the position of the level and its wave function.

## Acknowledgments

We thank A.V. Anisovich, Y.I. Azimov, G.S. Danilov, I.T. Dyatlov, L.N. Lipatov, V.Y. Petrov, H.R. Petry and M.G. Ryskin for useful discussions.

This work was supported by the Russian Foundation for Basic Research, project no. 04-02-17091.

## 5 Appendix I. The structure of pseudoscalar, scalar and vector exchanges

The loop diagram, that includes the interaction, is given by the expression as follows:

$$Sp[Q_{\mu_1 \dots \mu_J}^{(S,L,J)}(m + \hat{k}_1)O_I(m + \hat{k}'_1)Q_{\nu_1 \dots \nu_J}^{(S,L,J)}(m - \hat{k}'_2)O_I(m - \hat{k}_2)] = V_I^{(S,L,J)}(-1)^J O_{\nu_1 \dots \nu_J}^{\mu_1 \dots \mu_J}, \quad (92)$$

where  $k_1, k_2$  are the momenta of particles before the interaction,  $k'_1, k'_2$  are their momenta after the interaction, and the operators  $O_I$ 's are given by (14).

For the singlet ( $S = 0$ ) states in the case of scalar, pseudoscalar and vector exchanges, we obtain:

$$\begin{aligned} V_I^{(0,J,J)} &= \sqrt{ss'}(4z\kappa - 4m^2 - \sqrt{ss'})\kappa^J P_J(z), \\ V_{\gamma_5}^{(0,J,J)} &= \sqrt{ss'}(4z\kappa + 4m^2 - \sqrt{ss'})\kappa^J P_J(z), \\ V_{\gamma_\mu}^{(0,J,J)} &= \sqrt{ss'}(4\sqrt{ss'} - 8m^2)\kappa^J P_J(z). \end{aligned} \quad (93)$$

Here,  $P_J(z)$  are Legendre polynomials depending on the angle between final and initial particles and

$$\kappa = |\mathbf{k}||\mathbf{k}'|. \quad (94)$$

Near the threshold, the pseudoscalar interaction has a higher order factors  $\kappa |\mathbf{k}||\mathbf{k}'|$  than in the case of scalar and vector interactions thus playing a minor role for mesons consisted of heavy quarks. The scalar and vector interactions in the lowest  $|\mathbf{k}||\mathbf{k}'|$  order are equal to each other in absolute value but have opposite sign.

To obtain the expressions for triplet states, first, let us calculate the trace with vertex functions taken as  $\gamma_\mu$ . Then, general expression can be obtained by the convolution of the trace operators:

$$\begin{aligned} Sp[\gamma_\mu(m + \hat{k}_1)O_I(m + \hat{k}'_1)\gamma_\nu(m - \hat{k}'_2)O_I(m - \hat{k}_2)] &= (a_1^I + z\kappa a_2^I)g_{\mu\nu}^\perp + a_3^I k_\mu^\perp k_\nu^\perp + \\ &+ a_4^I k_\mu'^\perp k_\nu'^\perp + (a_5^I + z\kappa a_6^I)k_\mu^\perp k_\nu'^\perp + a_7^I(k_\mu^\perp k_\nu'^\perp - k_\mu'^\perp k_\nu^\perp). \end{aligned} \quad (95)$$

The coefficients  $a_i$  for the scalar, pseudoscalar and vector exchanges are equal to

$O_I$	1	$\gamma_5$	$\gamma_\mu$
$a_1^I$	$\sqrt{ss'}(4m^2 + \sqrt{ss'})$	$\sqrt{ss'}(4m^2 - \sqrt{ss'})$	$-2ss'$
$a_2^I$	$-4\sqrt{ss'}$	$+4\sqrt{ss'}$	$-8\sqrt{ss'}$
$a_3^I$	$+4s'$	$-4s'$	$-8s'$
$a_4^I$	$+4s$	$-4s$	$-8s$
$a_5^I$	$4(4m^2 - \sqrt{ss'})$	$4(4m^2 + \sqrt{ss'})$	$8(8m^2 - \sqrt{ss'})$
$a_6^I$	$-16$	$+16$	$+32$
$a_7^I$	$+4\sqrt{ss'}$	$-4\sqrt{ss'}$	$+8\sqrt{ss'}$

(96)

Then, for  $S = 1$  and  $L = J$  states we obtain:

$$\begin{aligned}
V_1^{(1,J,J)} &= \sqrt{ss'}\kappa^J \left[ (4z\kappa - 4m^2 - \sqrt{ss'})P_J(z) - \frac{4\kappa}{J+1}(zP_J(z) - P_{J-1}(z)) \right], \\
V_{\gamma_5}^{(1,J,J)} &= \sqrt{ss'}\kappa^J \left[ (-4z\kappa - 4m^2 + \sqrt{ss'})P_J(z) + \frac{4\kappa}{J+1}(zP_J(z) - P_{J-1}(z)) \right], \\
V_{\gamma_\mu}^{(1,J,J)} &= \sqrt{ss'}\kappa^J \left[ (2\sqrt{ss'} + 8z\kappa)P_J(z) - \frac{8\kappa}{J+1}(zP_J(z) - P_{J-1}(z)) \right].
\end{aligned}
\tag{97}$$

Likewise, the states with  $L = J \pm 1$  are expressed as follows:

$$V_I^{(1,L,L',J)} = \frac{-1}{2J+1} \kappa^{\frac{L+L'}{2}} \sum_{k=1}^7 a_k^I v_k^{(L,L')}.
\tag{98}$$

We use additional index ( $L'$ ) to describe transitions between states with  $L^+ = J+1$  and  $L^- = J-1$ .

	$L^- \rightarrow L^-$	$L^+ \rightarrow L^+$	$L^- \rightarrow L^+$	$L^+ \rightarrow L^-$
$v_1^{(L,L')}$	$(2J+1)P_{J-1}(z)$	$(2J+1)P_{J+1}(z)$	0	0
$v_2^{(L,L')}$	$(2J+1)z\kappa P_{J-1}(z)$	$(2J+1)z\kappa P_{J+1}(z)$	0	0
$v_3^{(L,L')}$	$-JP_{J-1}(z) \mathbf{k} ^2$	$-(J+1)P_{J+1}(z) \mathbf{k} ^2$	$\Lambda \kappa P_{J+1}$	$\Lambda P_{J-1} \frac{ \mathbf{k} ^4}{\kappa}$
$v_4^{(L,L')}$	$-JP_{J-1}(z) \mathbf{k}' ^2$	$-(J+1)P_{J+1}(z) \mathbf{k}' ^2$	$\Lambda P_{J-1}(z) \frac{ \mathbf{k}' ^4}{\kappa}$	$\Lambda \kappa P_{J+1}(z)$
$v_5^{(L,L')}$	$-J\kappa P_J(z)$	$-(J+1)\kappa P_J(z)$	$\Lambda P_J(z) \mathbf{k}' ^2$	$\Lambda P_J(z) \mathbf{k} ^2$
$v_6^{(L,L')}$	$-Jz\kappa^2 P_J(z)$	$-(J+1)z\kappa^2 P_J(z)$	$\Lambda z\kappa P_J(z) \mathbf{k}' ^2$	$\Lambda z\kappa P_J(z) \mathbf{k} ^2$
$v_7^{(L,L')}$	$\frac{(2J+1)(1-J)}{2J-1} \kappa (P_J(z) - P_{J-2}(z))$	$(2J+1)\kappa (zP_{J+1}(z) - P_J(z))$	0	0

(99)

Here,  $\Lambda = \sqrt{J(J+1)}$  and  $\kappa$  are defined by (94).

## 6 Appendix II. Wave functions in the $b\bar{b}$ sector

The tables 1–4 demonstrate the coefficient values  $c_i^{(n)}$ , which determine the wave functions  $\psi^{(S,L,J)}$  according to (77). In the tables we also show  $W_{LL'}$ , which determine the normalization condition, see (13). In Figs. 6–9, we demonstrate these wave functions.



Table 1: Constants  $c_i^{(n)}$  from (77) (in GeV) for the wave functions of the  $\Upsilon$ -mesons in solution  $I(b\bar{b})$ ; also we present the normalization coefficients  $W_{00}, W_{02}, W_{22}$  given by (12),(13).

	$\Upsilon(1S)$			$\Upsilon(2S)$			$\Upsilon(3S)$		
	$W_{00}$	$W_{02}$	$W_{22}$	$W_{00}$	$W_{02}$	$W_{22}$	$W_{00}$	$W_{02}$	$W_{22}$
	1.00050	-0.00060	0.00010	1.00101	-0.00122	0.00021	1.00115	-0.00143	0.00028
$i$	$\psi^{(1,0,1)}$	$\psi^{(1,2,1)}$	$\psi^{(1,0,1)}$	$\psi^{(1,2,1)}$	$\psi^{(1,0,1)}$	$\psi^{(1,2,1)}$	$\psi^{(1,0,1)}$	$\psi^{(1,2,1)}$	$\psi^{(1,2,1)}$
1	2.0060	-1.9545	2.7111	1.7177	-4.7273	1.9830			
2	-10.8380	13.5543	9.8323	-12.2344	9.5837	-12.8048			
3	73.0097	-36.0805	-72.4706	32.3653	-52.0435	33.3246			
4	-230.4699	47.0494	221.2708	-41.5308	240.2794	-42.7176			
5	397.0086	-30.8840	-386.7066	26.4284	-457.6044	26.8052			
6	-389.9981	7.9660	386.9034	-6.1016	453.3999	-5.5935			
7	218.1722	1.2842	-219.7120	-1.5700	-251.5948	-2.0591			
8	-64.5122	-1.1142	65.7237	1.0735	73.9804	1.2288			
9	7.8476	0.1657	-8.0769	-0.1519	-9.0153	-0.1688			
	$\Upsilon(4S)$			$\Upsilon(5S)$			$\Upsilon(6S)$		
	$W_{00}$	$W_{02}$	$W_{22}$	$W_{00}$	$W_{02}$	$W_{22}$	$W_{00}$	$W_{02}$	$W_{22}$
	1.00118	-0.00155	0.00037	1.00149	-0.00185	0.00036	0.80131	0.03464	0.16405
$i$	$\psi^{(1,0,1)}$	$\psi^{(1,2,1)}$	$\psi^{(1,0,1)}$	$\psi^{(1,2,1)}$	$\psi^{(1,0,1)}$	$\psi^{(1,2,1)}$	$\psi^{(1,0,1)}$	$\psi^{(1,2,1)}$	$\psi^{(1,2,1)}$
1	-4.6053	-1.9248	4.7469	-2.3093	4.3499	-33.8613			
2	-12.9581	16.3285	26.3926	11.4831	66.6334	71.5349			
3	122.1101	-45.3030	-218.0913	-23.7269	-672.1165	95.8832			
4	-232.1932	57.4674	306.9638	26.0199	2023.7316	-345.3417			
5	242.2475	-34.4863	140.7892	-15.4406	-2851.3726	273.7456			
6	-211.8979	6.2974	-597.4634	3.9824	2118.8719	-24.6291			
7	139.6440	2.9879	479.8989	0.3477	-850.6343	-61.8950			
8	-50.5914	-1.5944	-161.4547	-0.4002	175.5466	27.9503			
9	7.2976	0.2100	20.2973	0.0570	-15.0191	-3.6706			

Table 2: Constants  $c_i^{(n)}$  from eq. (77) (in GeV units) for the wave functions of  $\Upsilon$ -mesons in the solution  $I(b\bar{b})$ ; normalization coefficients  $W_{00}, W_{02}, W_{22}$  are given by (12),(13).

	$\Upsilon(1D)$			$\Upsilon(2D)$			$\Upsilon(3D)$		
	$W_{00}$	$W_{02}$	$W_{22}$	$W_{00}$	$W_{02}$	$W_{22}$	$W_{00}$	$W_{02}$	$W_{22}$
	0.00083	-0.00214	1.00131	0.00144	-0.00360	1.00217	0.00210	-0.00499	1.00290
$i$	$\psi^{(1,2,1)}$	$\psi^{(1,0,1)}$	$\psi^{(1,2,1)}$	$\psi^{(1,0,1)}$	$\psi^{(1,2,1)}$	$\psi^{(1,0,1)}$	$\psi^{(1,2,1)}$	$\psi^{(1,0,1)}$	$\psi^{(1,2,1)}$
1	0.5316	0.0051	-14.2711	-0.0804	6.0089	0.0734			
2	22.2640	0.2961	29.5676	0.4676	104.3726	0.4895			
3	-61.8266	-2.1943	-62.5673	-3.1827	-367.7237	-4.4838			
4	79.4272	7.1306	100.0037	11.9276	446.4882	12.5128			
5	-50.4830	-12.7875	-73.1973	-21.9636	-236.8819	-20.8090			
6	10.6083	12.9455	15.1171	22.1691	31.8558	22.5104			
7	4.5874	-7.4078	8.7956	-12.6656	23.2527	-14.3861			
8	-2.8530	2.2290	-5.1628	3.8222	-10.8663	4.7718			
9	0.4300	-0.2751	0.7691	-0.4749	1.4288	-0.6355			
	$\Upsilon(4D)$			$\Upsilon(5D)$			$\Upsilon(6D)$		
	$W_{00}$	$W_{02}$	$W_{22}$	$W_{00}$	$W_{02}$	$W_{22}$	$W_{00}$	$W_{02}$	$W_{22}$
	0.00230	-0.00585	1.00355	0.20433	-0.04594	0.84162	0.00126	-0.00134	1.00008
$i$	$\psi^{(1,2,1)}$	$\psi^{(1,0,1)}$	$\psi^{(1,2,1)}$	$\psi^{(1,0,1)}$	$\psi^{(1,2,1)}$	$\psi^{(1,0,1)}$	$\psi^{(1,2,1)}$	$\psi^{(1,0,1)}$	$\psi^{(1,2,1)}$
1	-32.4189	-0.0913	80.9176	2.0418	-377.8732	0.5165			
2	-32.2563	-0.3537	-211.1041	33.2603	2121.7911	-1.1281			
3	385.0197	1.9186	-54.4316	-333.9307	-4529.4955	-14.6612			
4	-592.6611	6.0232	550.7145	1012.1198	4646.2765	69.2347			
5	321.7644	-30.8630	-476.3406	-1440.4555	-2245.1955	-123.0232			
6	-16.3314	44.9067	41.8114	1084.8218	251.1282	109.8199			
7	-45.1952	-29.9473	113.3274	-443.3884	204.4454	-52.1311			
8	15.1386	9.5444	-50.9272	93.7641	-81.9575	12.5435			
9	-1.4251	-1.1922	6.6630	-8.2835	9.2592	-1.2099			

Table 3: Constants  $c_i^{(n)}$  from (77) (in GeV) for the wave functions of  $\chi_{b2}$ -mesons in the solution  $I(b\bar{b})$  normalization coefficients  $W_{00}, W_{02}, W_{22}$  are given by (12),(13).

		$\chi_{b2}(1P)$			$\chi_{b2}(2P)$			$\chi_{b2}(3P)$		
		$W_{11}$	$W_{13}$	$W_{33}$	$W_{11}$	$W_{13}$	$W_{33}$	$W_{11}$	$W_{13}$	$W_{33}$
		1.00075	-0.00094	0.00019	1.00128	-0.00203	0.00075	0.98981	-0.00494	0.01514
$i$		$\psi^{(1,1,2)}$	$\psi^{(1,3,2)}$	$\psi^{(1,1,2)}$	$\psi^{(1,3,2)}$	$\psi^{(1,1,2)}$	$\psi^{(1,3,2)}$	$\psi^{(1,1,2)}$	$\psi^{(1,3,2)}$	$\psi^{(1,3,2)}$
1		13.0540	-4.1772	-34.6278	16.0313	-257.7504	100.2644			
2		-114.9374	23.4967	456.0158	-90.5844	2844.0283	-561.9424			
3		487.8876	-52.5492	-1939.7651	201.0440	-12019.5471	1240.5753			
4		-1062.2386	60.1441	4168.0416	-227.9811	25892.6834	-1399.5333			
5		1317.9252	-37.5852	-5113.9135	141.4654	-31653.5893	863.3132			
6		-967.3832	12.2496	3712.1978	-46.2459	22808.4240	-280.4788			
7		414.8491	-1.5240	-1571.7829	6.1338	-9564.2325	37.0697			
8		-95.8539	-0.1252	357.7836	0.2835	2152.2305	1.6274			
9		9.2113	0.0356	-33.7704	-0.1074	-200.3714	-0.6277			
		$\chi_{b2}(4P)$			$\chi_{b2}(5P)$			$\chi_{b2}(6P)$		
		$W_{11}$	$W_{13}$	$W_{33}$	$W_{11}$	$W_{13}$	$W_{33}$	$W_{11}$	$W_{13}$	$W_{33}$
		1.00071	-0.00246	0.00176	1.00246	-0.00318	0.00072	1.00311	-0.00397	0.00086
$i$		$\psi^{(1,1,2)}$	$\psi^{(1,3,2)}$	$\psi^{(1,1,2)}$	$\psi^{(1,3,2)}$	$\psi^{(1,1,2)}$	$\psi^{(1,3,2)}$	$\psi^{(1,1,2)}$	$\psi^{(1,3,2)}$	$\psi^{(1,3,2)}$
1		61.1310	-27.9538	-21.7721	4.7026	10.8365	-2.3155			
2		-804.3179	157.6290	68.2854	-23.9703	144.6924	5.6067			
3		3433.8802	-347.3610	-194.8198	48.5937	-929.0568	2.8923			
4		-7271.1541	388.8039	630.5268	-51.7634	1868.8590	-20.3080			
5		8755.3125	-236.5028	-1080.4598	32.0724	-1686.1180	23.4272			
6		-6242.9707	74.8939	933.0968	-12.0176	679.5364	-11.5459			
7		2595.9632	-9.1414	-421.0616	2.7404	-61.8407	2.2550			
8		-579.2785	-0.6539	94.9352	-0.3698	-31.7481	0.0334			
9		53.3862	0.1874	-8.3610	0.0242	6.7593	-0.0471			
		$\chi_{b2}(1F)$			$\chi_{b2}(2F)$			$\chi_{b2}(3F)$		
		$W_{11}$	$W_{13}$	$W_{33}$	$W_{11}$	$W_{13}$	$W_{33}$	$W_{11}$	$W_{13}$	$W_{33}$
		0.00058	-0.00191	1.00132	0.00097	-0.00315	1.00218	0.00124	-0.00390	1.00266
$i$		$\psi^{(1,3,2)}$	$\psi^{(1,1,2)}$	$\psi^{(1,3,2)}$	$\psi^{(1,1,2)}$	$\psi^{(1,3,2)}$	$\psi^{(1,1,2)}$	$\psi^{(1,3,2)}$	$\psi^{(1,1,2)}$	$\psi^{(1,1,2)}$
1		-3.6248	-0.0963	-14.7982	0.0560	-37.1706	2.9107			
2		-7.2244	0.8055	0.1033	-1.0323	9.5966	-34.8030			
3		19.9292	-2.9097	31.5118	3.4274	147.9125	151.9065			
4		-17.8259	5.3091	-19.0518	-4.1874	-177.1377	-332.1606			
5		5.4336	-5.0342	-2.9800	1.6200	36.1365	410.3068			
6		2.6649	2.4892	3.3342	1.1027	48.9104	-298.9169			
7		-2.9157	-0.5206	1.0840	-1.4679	-35.1616	126.9788			
8		0.9614	-0.0152	-0.9814	0.5902	9.1555	-29.0017			
9		-0.1144	0.0160	0.1614	-0.0846	-0.8818	2.7474			
		$\chi_{b2}(4F)$			$\chi_{b2}(5F)$			$\chi_{b2}(6F)$		
		$W_{11}$	$W_{13}$	$W_{33}$	$W_{11}$	$W_{13}$	$W_{33}$	$W_{11}$	$W_{13}$	$W_{33}$
		0.00244	-0.00497	1.00253	0.00119	-0.00465	1.00346	0.20223	0.04827	0.74950
$i$		$\psi^{(1,3,2)}$	$\psi^{(1,1,2)}$	$\psi^{(1,3,2)}$	$\psi^{(1,1,2)}$	$\psi^{(1,3,2)}$	$\psi^{(1,1,2)}$	$\psi^{(1,3,2)}$	$\psi^{(1,1,2)}$	$\psi^{(1,1,2)}$
1		137.2096	-3.9590	-295.5265	0.0318	-342.8625	88.3149			
2		-395.5970	55.7513	1172.2960	-8.1102	1605.5381	-670.5111			
3		346.9297	-259.4898	-1660.4991	60.4182	-2779.6979	1944.5425			
4		-64.2683	578.6142	946.4669	-176.4908	2084.3230	-2837.7766			
5		-14.0966	-709.0203	-65.5667	263.0556	-374.7669	2282.8464			
6		-40.3793	502.8571	-139.7540	-217.9552	-406.6671	-1033.5668			
7		38.2866	-205.4367	44.2943	101.2739	272.3230	257.4060			
8		-11.2262	44.7930	-0.5172	-24.6525	-64.5095	-33.5769			
9		1.0954	-4.0251	-0.8887	2.4484	5.5083	2.1172			

Table 4: Constants  $c_i^{(n)}$  from (85) (in GeV) for wave functions  $\eta_{b0}$ ,  $\chi_{b0}$ ,  $\chi_{b1}$  and  $h_{b1}$  in solution  $I(b\bar{b})$

$i$	$\eta_{b0}(1P)$	$\eta_{b0}(2P)$	$\eta_{b0}(3P)$	$\eta_{b0}(4P)$	$\eta_{b0}(5P)$	$\eta_{b0}(6P)$
1	4.5338	-1.1326	11.9074	-18.3892	29.5281	-3.5400
2	-55.4035	73.3964	-136.8130	411.7847	-480.8391	201.4420
3	329.9544	-440.1212	798.7926	-2495.6136	2863.6920	-1321.6947
4	-942.3382	1240.9035	-2311.1680	6933.5200	-8155.6641	3472.8097
5	1474.8959	-1923.5277	3573.4205	-10437.4060	12468.2246	-4685.6254
6	-1326.7453	1712.0637	-3132.4041	9006.4575	-10761.0759	3555.8036
7	682.8131	-870.3125	1560.9990	-4427.9932	5234.8626	-1537.4724
8	-186.4237	234.3339	-411.2328	1148.6087	-1334.8254	352.9427
9	20.9478	-25.9307	44.4414	-121.6868	138.3033	-33.1141
$i$	$\chi_{b0}(1P)$	$\chi_{b0}(2P)$	$\chi_{b0}(3P)$	$\chi_{b0}(4P)$	$\chi_{b0}(5P)$	$\chi_{b0}(6P)$
1	29.2420	-61.6937	-219.3775	126.2557	-42.4376	-6.8271
2	-304.0472	755.4596	2411.7486	-1536.0712	316.4890	347.2500
3	1304.2479	-3236.5223	-10285.1211	6586.8209	-1275.2749	-1772.0896
4	-2863.9307	7047.5098	22382.0814	-14186.9213	2956.9372	3636.4974
5	3585.8612	-8744.9017	-27622.3384	17341.7384	-3876.4948	-3793.2353
6	-2656.7748	6413.5855	20084.3830	-12510.0465	2897.0308	2166.3382
7	1149.8200	-2743.1742	-8497.3906	5252.0887	-1220.4556	-673.3240
8	-268.0686	630.9120	1929.4613	-1182.3208	268.9864	102.7608
9	25.9818	-60.1922	-181.3145	109.9412	-23.9653	-5.3795
$i$	$\chi_{b1}(1P)$	$\chi_{b1}(2P)$	$\chi_{b1}(3P)$	$\chi_{b1}(4P)$	$\chi_{b1}(5P)$	$\chi_{b1}(6P)$
1	33.0397	239.7994	-164.4051	34.1495	26.9515	8.4967
2	-332.6519	-2634.9469	1721.8106	-485.7810	-126.6739	149.8510
3	1385.1827	10912.2385	-7107.3970	2029.1900	430.9352	-885.8464
4	-2958.4499	-23096.8480	15028.0903	-4151.1836	-1094.3863	1678.5809
5	3605.9605	27851.8047	-18066.4365	4843.3153	1580.6111	-1375.8433
6	-2602.3368	-19853.0333	12821.3870	-3359.3446	-1243.8826	421.1791
7	1097.2744	8252.3736	-5300.9385	1361.1611	531.5536	55.6201
8	-249.2044	-1843.7114	1176.8983	-295.8920	-115.6049	-59.6685
9	23.5136	170.6412	-108.1134	26.4999	9.9105	9.4863
$i$	$h_b(1P)$	$h_b(2P)$	$h_b(3P)$	$h_b(4P)$	$h_b(5P)$	$h_b(6P)$
1	-26.9406	245.4519	-158.2896	29.3812	24.3700	10.9592
2	265.1898	-2696.0191	1654.8622	-435.3349	-96.8333	123.8420
3	-1104.2180	11165.1311	-6832.1653	1822.9779	306.2952	-785.0079
4	2358.6741	-23627.7741	14450.3845	-3718.3930	-838.9663	1479.3562
5	-2874.8697	28482.8717	-17375.2937	4327.6261	1290.5769	-1149.1916
6	2074.5354	-20294.0610	12332.5098	-2998.2763	-1052.4158	266.7467
7	-874.6420	8431.1444	-5099.3191	1214.5985	458.5851	117.4293
8	198.6257	-1882.4288	1132.2297	-264.0975	-100.7958	-72.9291
9	-18.7411	174.0887	-104.0177	23.6613	8.6824	10.6504

## References

- [1] A.V. Anisovich, V.V. Anisovich, B.N. Markov, M.A. Matveev, and A. V. Sarantsev, *Yad. Fiz.* **67**, 794 (2004) [*Phys. of Atomic Nuclei*, **67**, 773 (2004)].
- [2] V.V. Anisovich, M.N. Kobrinsky, J. Nyiri, Yu.M. Shabelski, "*Quark model and high energy collisions*", World Scientific, 2nd edition, 2004.
- [3] E. Salpeter and H.A. Bethe, *Phys. Rev.* **84**, 1232 (1951);  
E. Salpeter, *Phys. Rev.* **91**, 994 (1953).
- [4] D. Ebert, R.N. Faustov, and V.O. Galkin, *Phys. Rev. D* **67**, 014027 (2003).
- [5] R. Ricken, M. Koll, D. Merten, B.C. Metsch, and H.R. Petry, *Eur. Phys. J. A* **9**, 221 (2000).
- [6] J. Linde and H. Snellman, *Nucl. Phys. A* **619**, 346 (1997).
- [7] J. Resag and C.R. Münz, *Nucl. Phys. A* **590**, 735 (1995).
- [8] J.H. Kühn, preprint MPI-PAE/PTh 25/88 (1988).
- [9] A.V. Anisovich, V.V. Anisovich, and A.V. Sarantsev, *Phys. Rev. D* **62**, 051502(R) (2000).
- [10] E. Klempt, *Eur. Phys. J. C* **28** (2003).
- [11] U. Loering, B.C. Metsch, and H.R. Petry, *Eur. Phys. J. A* **10**, 447 (2001).
- [12] G. Parisi and R. Petronzio, *Phys. Lett. B* **94**, 51 (1980);  
M. Consoli and J.H. Field, *Phys. Rev. D* **49**, 1293 (1994).
- [13] J.M. Cornwell and J. Papavassiliou, *Phys. Rev. D* **40**, 3474 (1989).
- [14] V.V. Anisovich, S.M. Gerasyuta, and A.V. Sarantsev, *Int. J. Mod. Phys. A* **6**, 2625 (1991).
- [15] D.B. Leinweber *et al.*, *Phys. Rev. D* **58**, 031501 (1998).
- [16] C. Amsler, *Phys. Lett. B* **592**, 848 (2004).
- [17] V.V. Anisovich, M.N. Kobrinsky, D.I. Melikhov, and A.V. Sarantsev, *Nucl. Phys. A* **544**, 747 (1992);  
A.V. Anisovich and V.A. Sadovnikova, *Yad. Fiz.* **55**, 2657 (1992); **57**, 75 (1994); *Eur. Phys. J. A* **2**, 199 (1998).
- [18] V.V. Anisovich, D.I. Melikhov, and V.A. Nikonov, *Phys. Rev. D* **52**, 5295 (1995).
- [19] A.V. Anisovich, V.V. Anisovich, and V.A. Nikonov, *Eur. Phys. J. A* **12**, 103 (2001).
- [20] A.V. Anisovich, V.V. Anisovich, V.N. Markov, and V.A. Nikonov, *Yad. Fiz.* **65**, 523 (2002) [*Phys. Atom. Nucl.* **65**, 497 (2002)].

- [21] A.V. Anisovich, V.V. Anisovich, M.A. Matveev, and V.A. Nikonov, *Yad. Fiz.* **66**, 946 (2003) [*Phys. Atom. Nucl.* **66**, 914 (2003)].
- [22] V.V. Anisovich, D.I. Melikhov, and V.A. Nikonov, *Phys. Rev. D* **55**, 2918 (1997).
- [23] A.V. Anisovich, V.V. Anisovich, L.G. Dakhno, V.A. Nikonov, and A.V. Sarantsev, *Yad. Fiz.* **68**, 1892 (2005) [*Phys. Atom. Nucl.* **68**, 1830 (2005)];  
V.V. Anisovich, L.G. Dakhno, V.N. Markov, V.A. Nikonov, and A.V. Sarantsev, hep-ph/0410361 (2004).
- [24] G. Hulth and H. Snellman, *Phys. Rev D* **24**, 2978 (1981).
- [25] S. Godfrey and N. Isgur, *Phys. Rev. D* **32**, 189 (1985).
- [26] S.N. Gupta, S.F. Radford, and W.W. Repko, *Phys. Rev. D* **31**, 160 (1985).
- [27] W. Lucha, F. Schöberl, and D. Gromes, *Phys. Rep.* **200**, 127 (1991).
- [28] A.V. Anisovich, V.V. Anisovich, V.N. Markov, M.A. Matveev, and A.V. Sarantsev, *J. Phys. G: Nucl. Part. Phys.* **28**, 15 (2002).
- [29] H. Hertsbach, *Phys. Rev. C* **50**, 2562 (1994).
- [30] H. Hertsbach, *Phys. Rev. A* **46**, 3657 (1992).
- [31] F. Gross and J. Milana, *Phys. Rev. D* **43**, 2401 (1991).
- [32] K.M. Maung, D.E. Kahana, and J.W. Ng, *Phys. Rev. A* **46**, 3657 (1992).
- [33] A.V. Anisovich, V.V. Anisovich, V.N. Markov, M.A. Matveev, V.A. Nikonov and A.V. Sarantsev, hep-ph/0509042 (2005).
- [34] V.V. Anisovich and M.A. Matveev, *Yad. Fiz.* **67**, 634 (2004) [*Phys. Atom. Nucl.* **67**, 614 (2004)].
- [35] A.V. Anisovich, V.V. Anisovich, and V.A. Nikonov, hep-ph/0305216 (2003).
- [36] S. Eidelman, *et al.*, *Phys. Lett. B* **592**, 1 (2004).
- [37] V.V. Anisovich, L.G. Dakhno, B.N. Markov, and A. V. Sarantsev, hep-ph/0410361.
- [38] A.V. Manohar andp C.T. Sachrajda, *Phys. Rev. D* **66** , 010001-271 (2002).
- [39] P. González, *et. al.*, hep-ph/0409202 (2004).
- [40] D. Ebert, R.N. Faustov, and V.O. Galkin, *Phys. Rev D* **67**, 014027 (2003).
- [41] S.N. Münz, *Nucl. Phys. A* **609**, 364 (1996).
- [42] S.N. Gupta, S.F. Radford, and W.W. Repko, *Phys. Rev. D* **54**, 2075 (1996).

- [43] G.A. Schuler, F.A Berends, and R. van Gulik, Nucl. Phys. B **523**, 423 (1998).
- [44] H.-W. Huang, *et. al.*, Phys. Rev. D **54**, 2123 (1996); D **56**, 368 (1997).
- [45] E.S. Ackleh, T. Barnes *et. al.*, Phys. Rev. D **45**, 232 (1992).

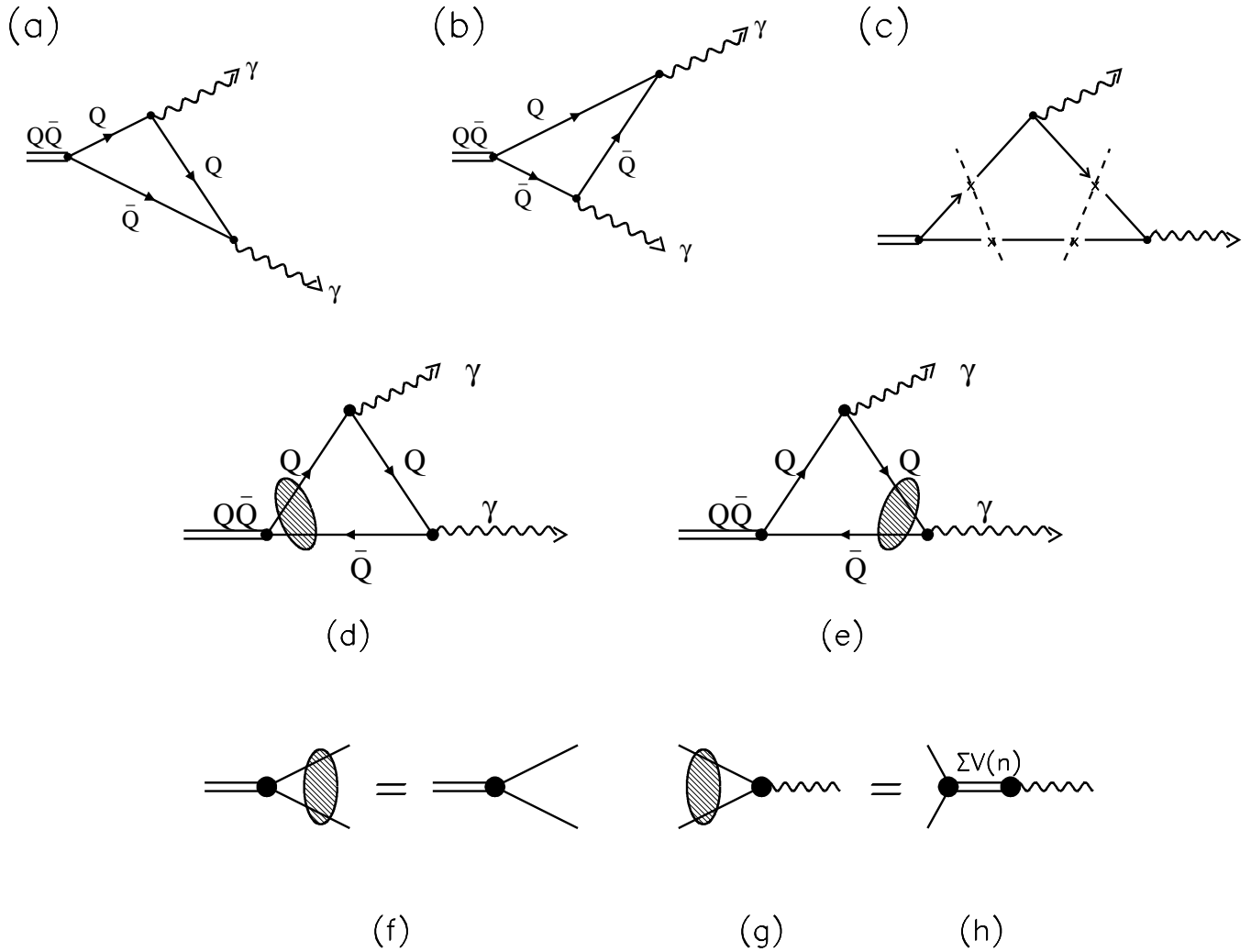


Figure 1: a,b) Diagrams for the two-photon decay of  $Q\bar{Q}$  state and c) cuttings in the spectral integral representation. Initial (d) and final (e) state interactions of quarks in the decay diagrams. f) Graphical representation of the spectral integral equation for the  $Q\bar{Q}$  vertex. g,h) Interaction of quarks in the vertex  $Q\bar{Q} \rightarrow \gamma$  and its approximation by the sum of transitions  $Q\bar{Q} \rightarrow \sum_n V(n) \rightarrow \gamma$ .



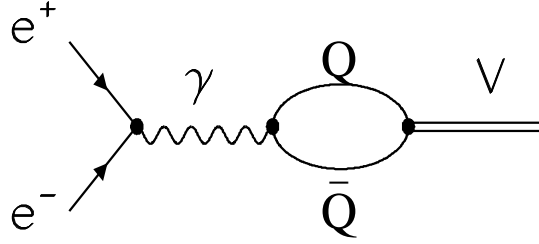


Figure 2: Quark transition diagram for the process  $e^+e^- \rightarrow V$ .

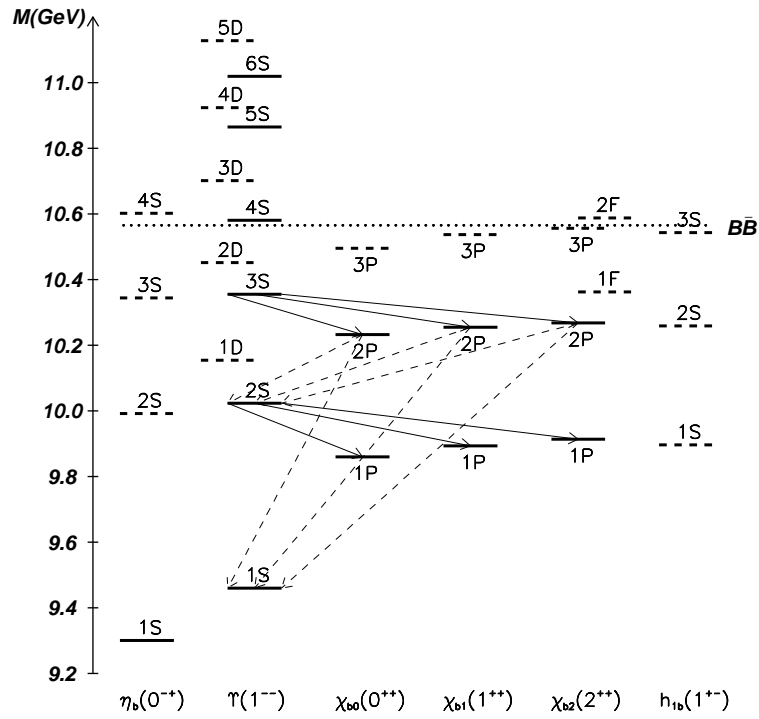


Figure 3: Radiative decays of the bottomonium systems, which were taken into account in the fit (solid lines). The dashed lines show radiative transitions with the known ratios for the branchings  $Br[\chi_{bJ}(2P) \rightarrow \gamma\Upsilon(2S)]/Br[\chi_{bJ}(2P) \rightarrow \gamma\Upsilon(1S)]$ , these ratios are not included in the fit.

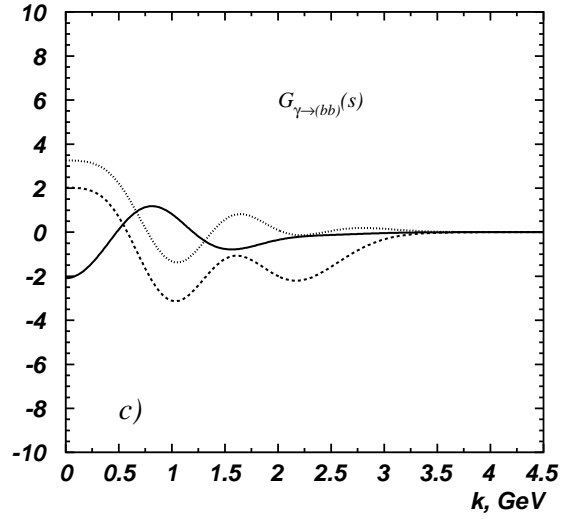
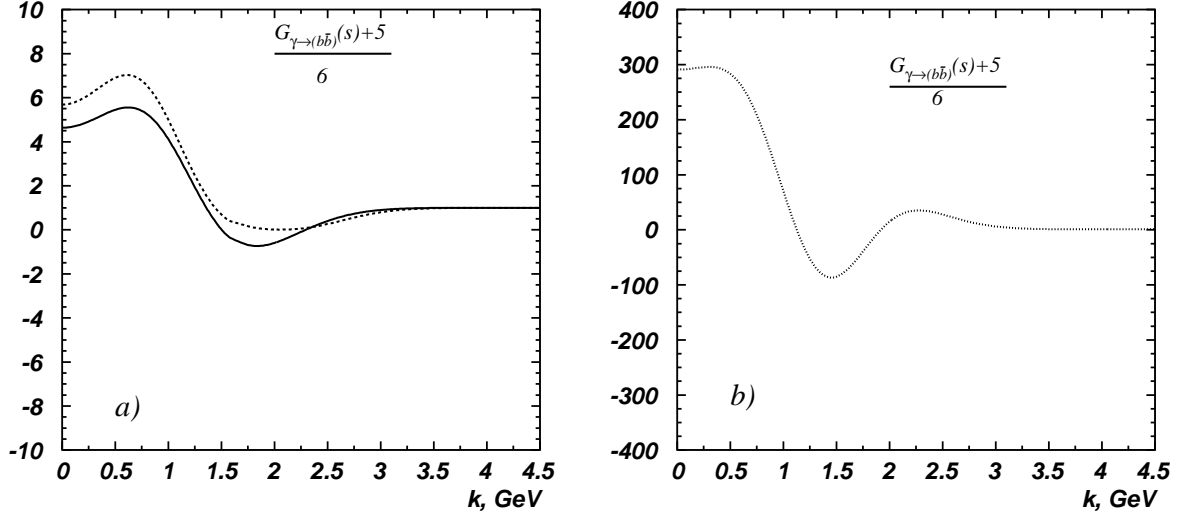


Figure 4: a) Vertices  $G_{\gamma \to b\bar{b}}^{(S)}$  (a) and  $G_{\gamma \to b\bar{b}}^{(D)}$  (b) for the solutions  $I(b\bar{b})$  (solid line),  $U(b\bar{b})$  (dash line) and  $R(b\bar{b})$  (dotted line).

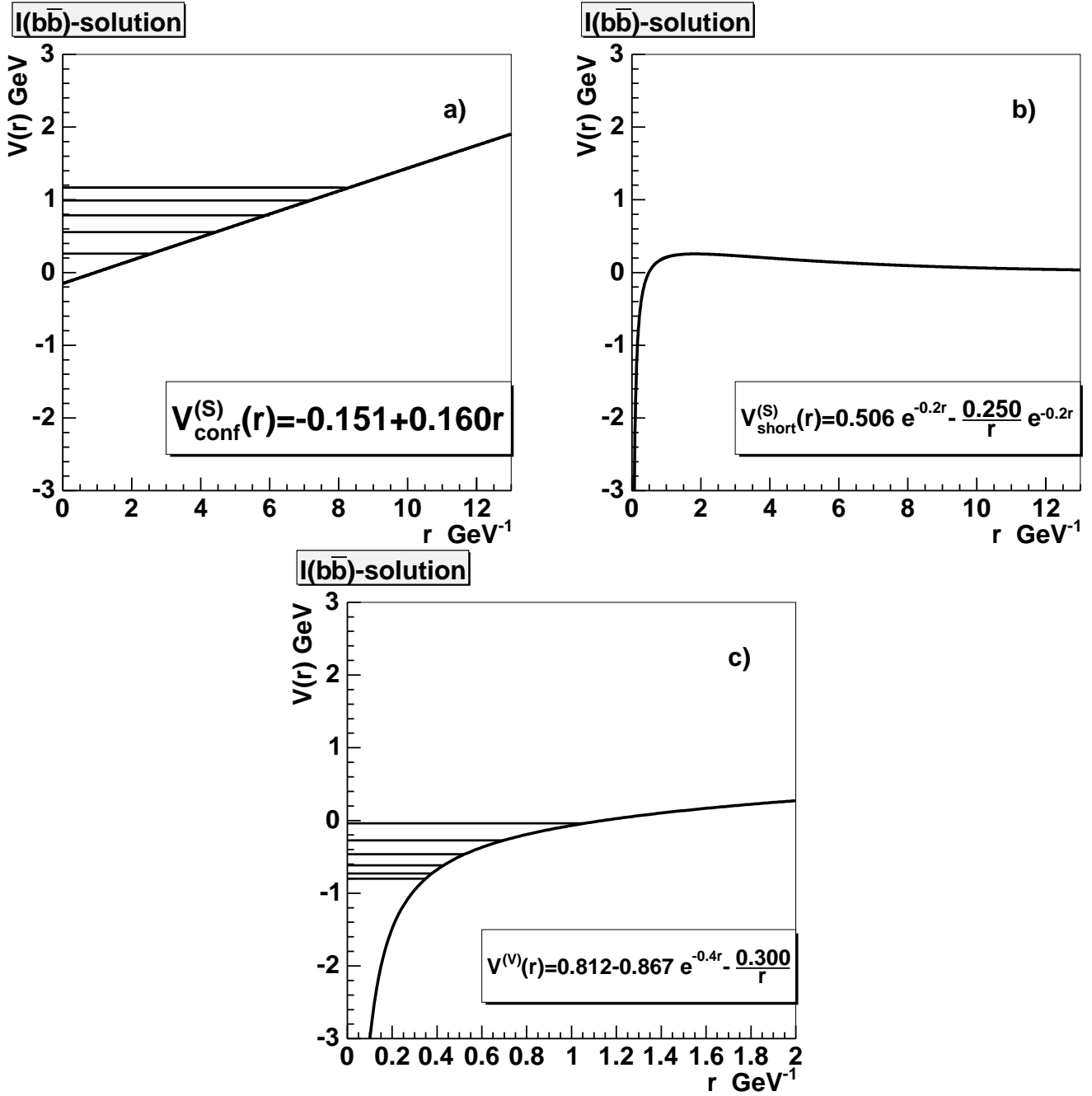


Figure 5: Potential for the solution  $I(b\bar{b})$ : confinement potential (a), short-range repulsive one (b) and attractive potential due to vector exchange (c). To be illustrative, we show the  $0^{-+}$  levels, which would be created by the attractive potentials.

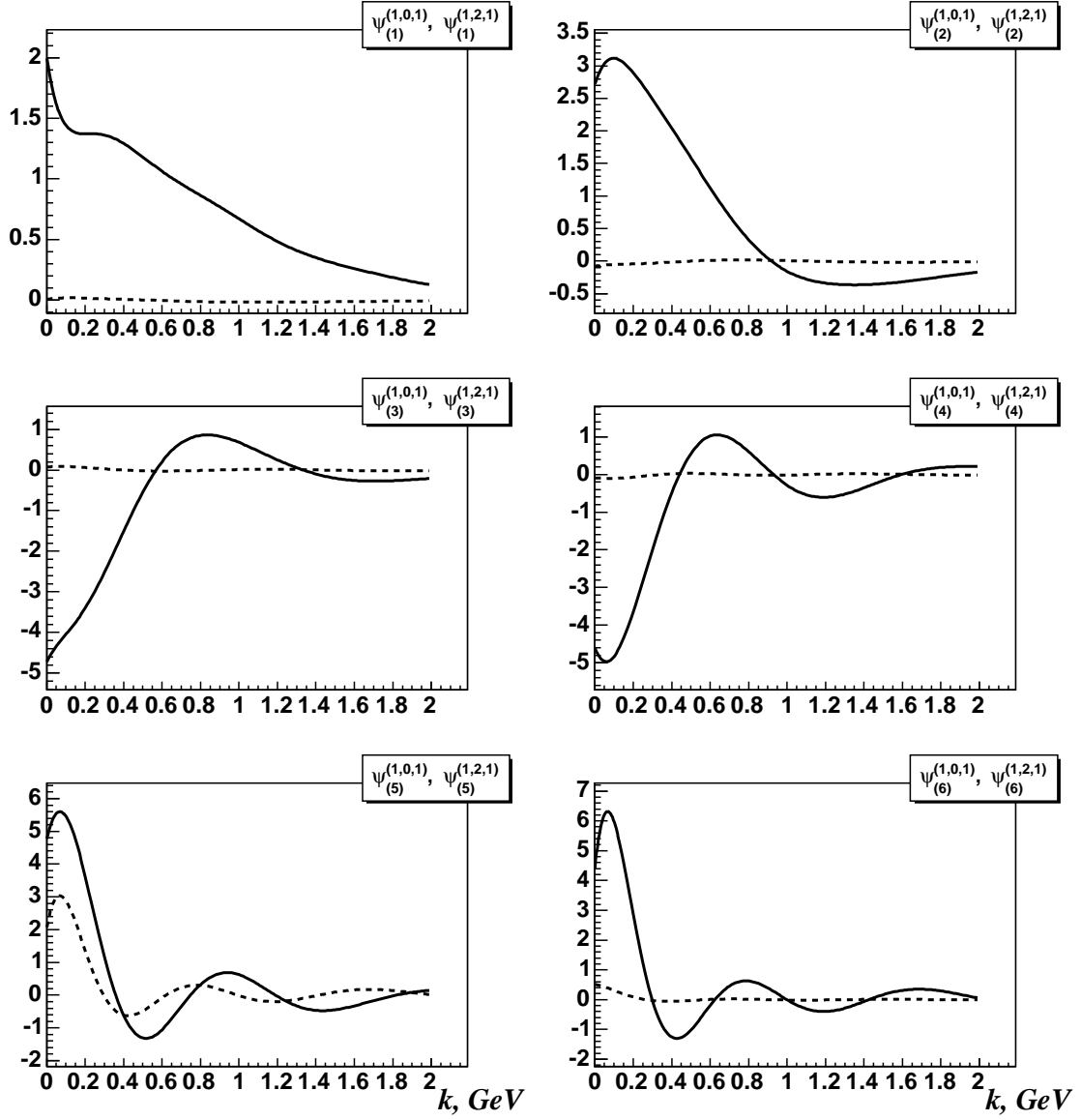


Figure 6: Wave functions for  $\Upsilon(nS)$  in the solution  $I(b\bar{b})$ . Solid and dashed lines stand for  $\psi^{(1,0,1)}$  and  $\psi^{(1,2,1)}$ .

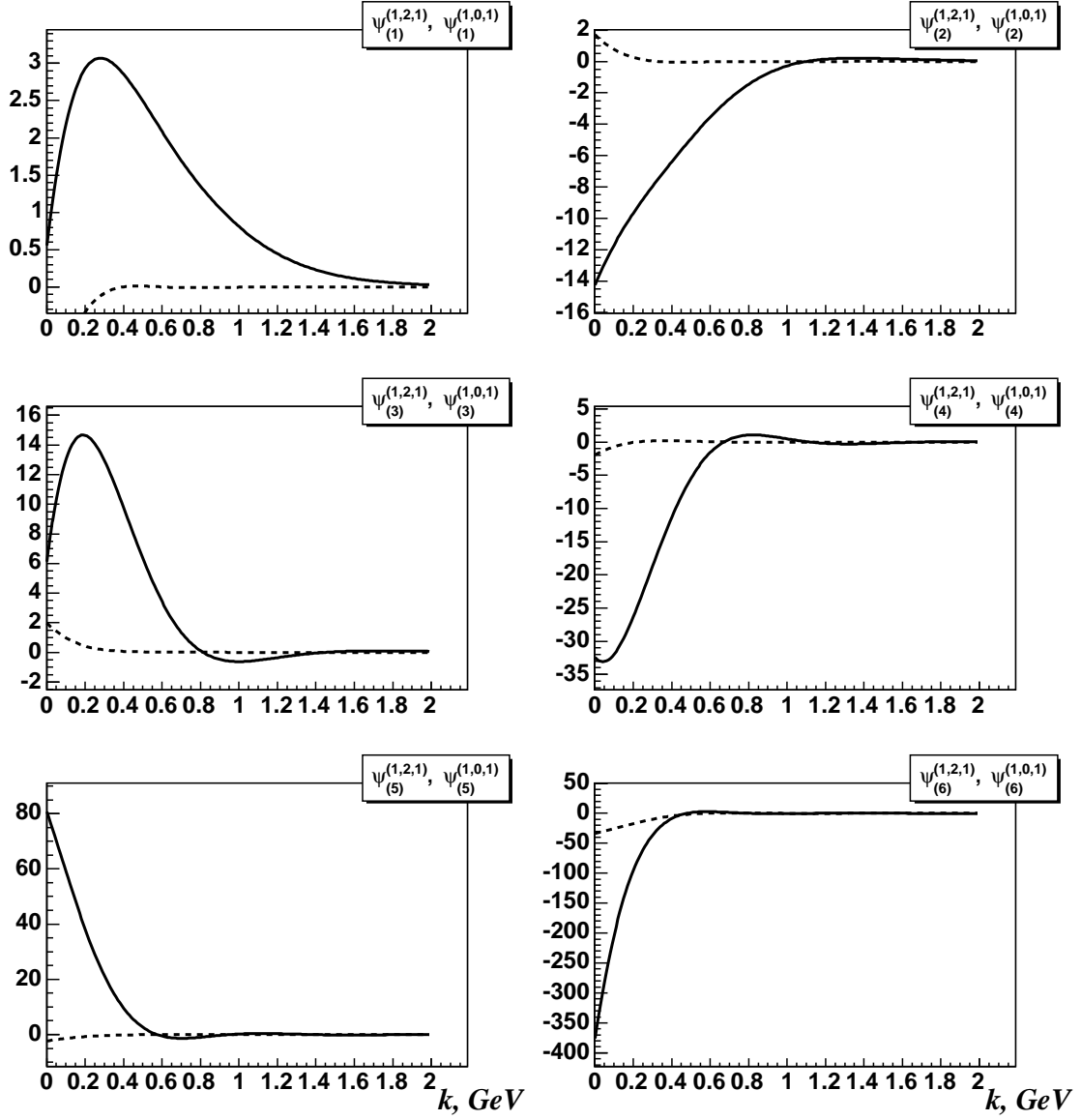


Figure 7: Wave functions for  $\Upsilon(nD)$  in the solution  $I(b\bar{b})$ . Solid and dashed lines stand for  $\psi^{(1,0,1)}$  and  $\psi^{(1,2,1)}$ .

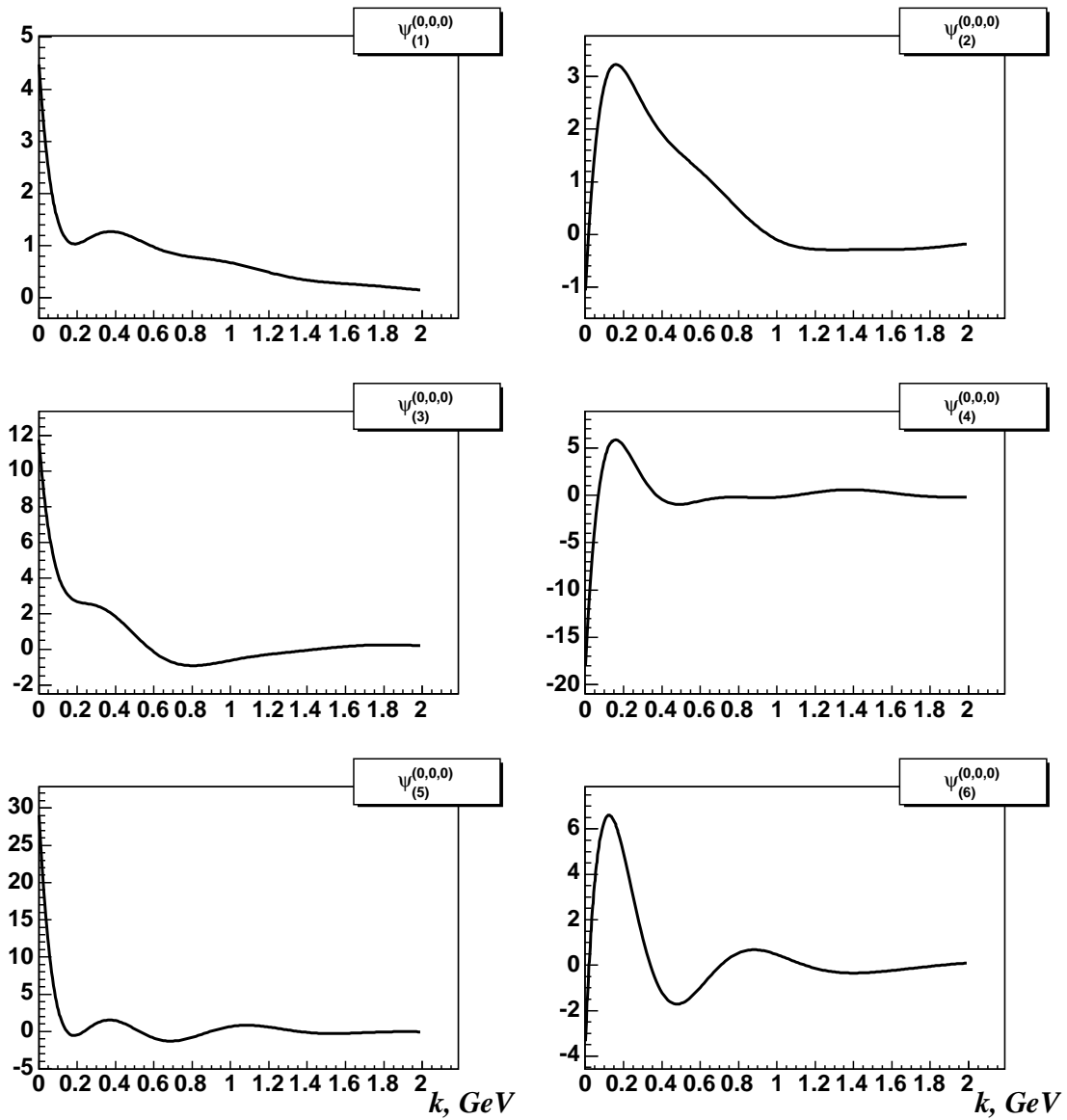


Figure 8: Wave functions for  $\eta_{b0}$  in the solution  $I(b\bar{b})$ .

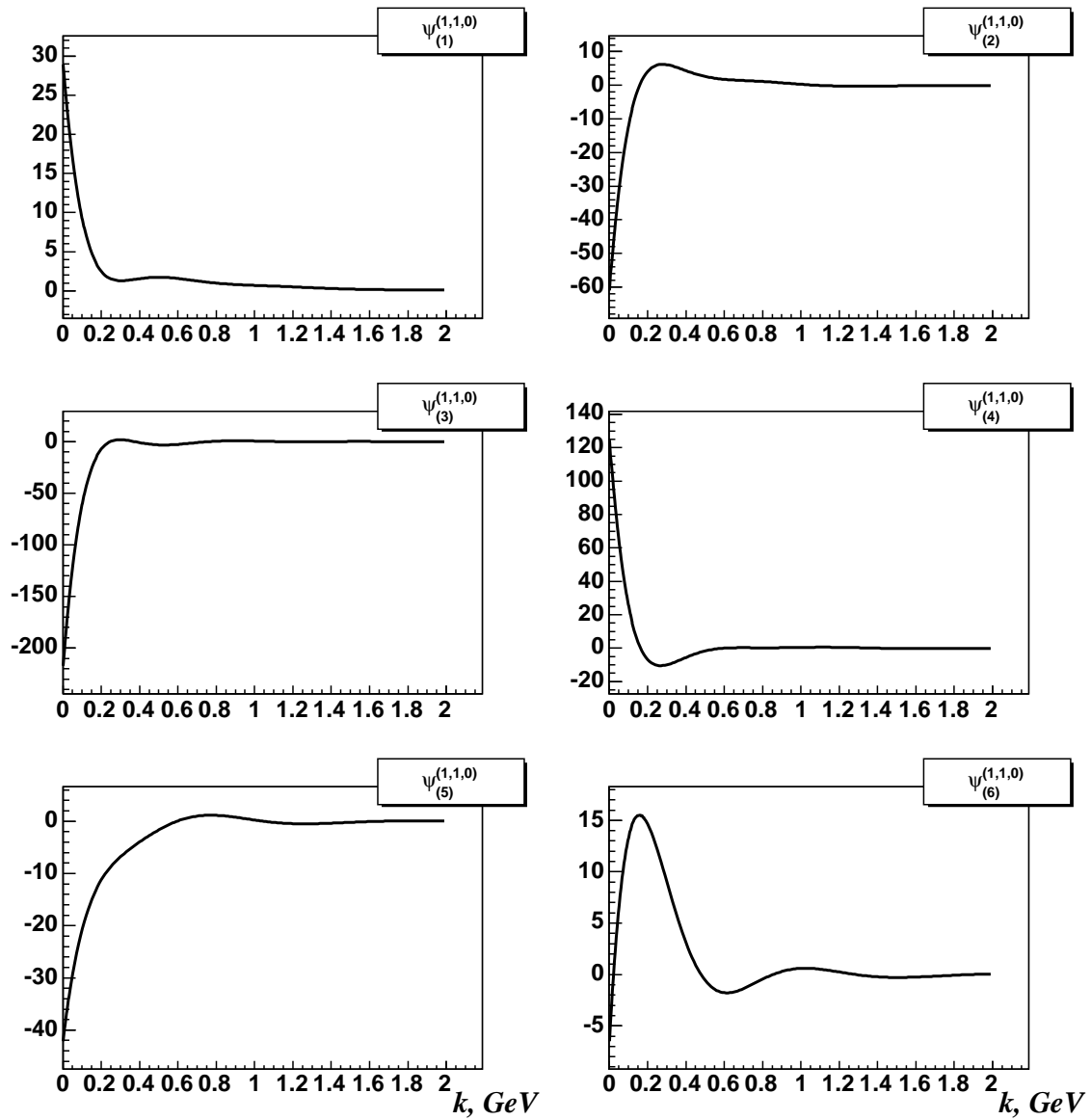


Figure 9: Wave functions for  $\chi_{b0}$  in the solution  $I(b\bar{b})$ .

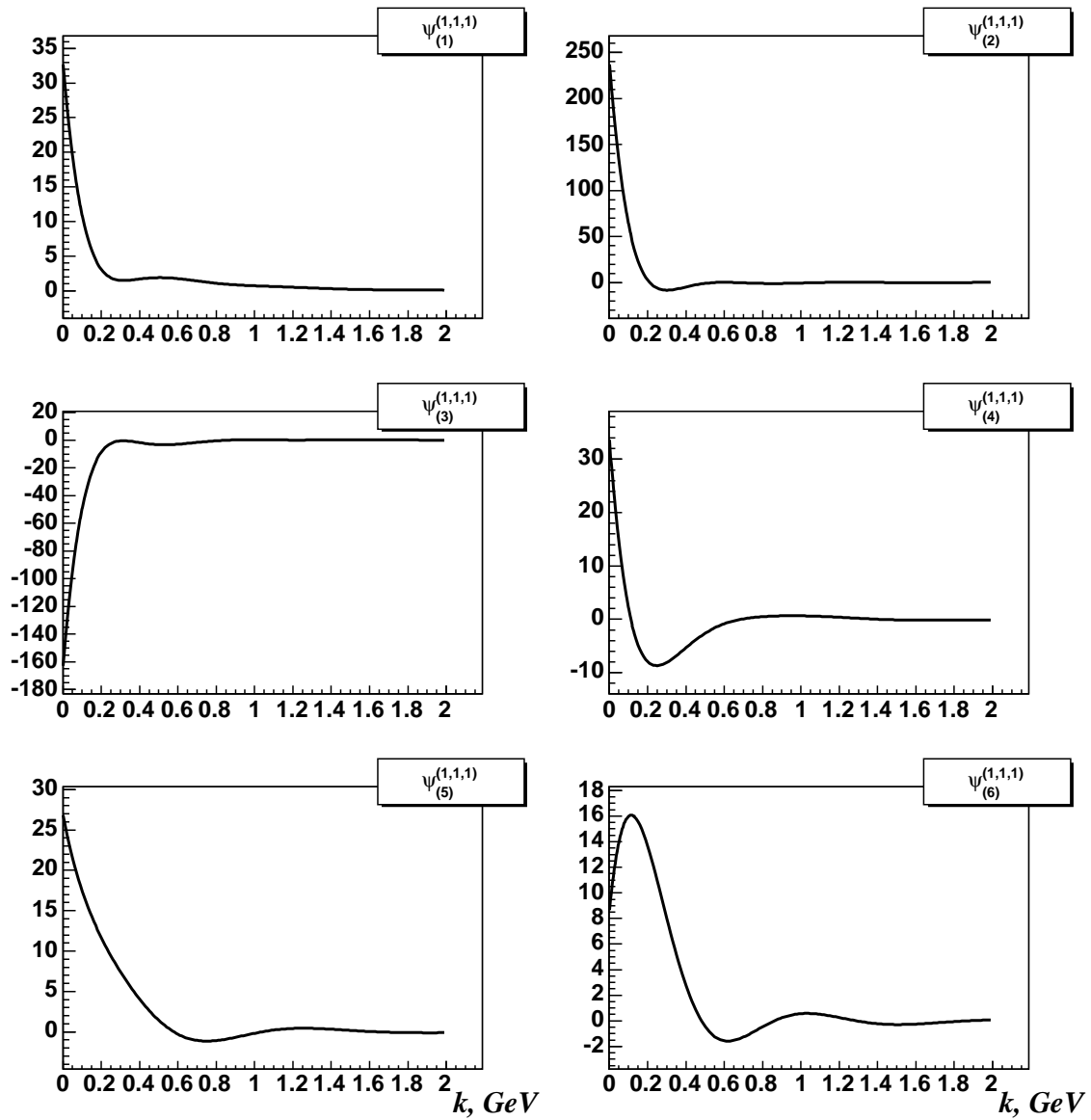


Figure 10: Wave functions for  $\chi_{b1}$  for the solutions  $I(b\bar{b})$ .



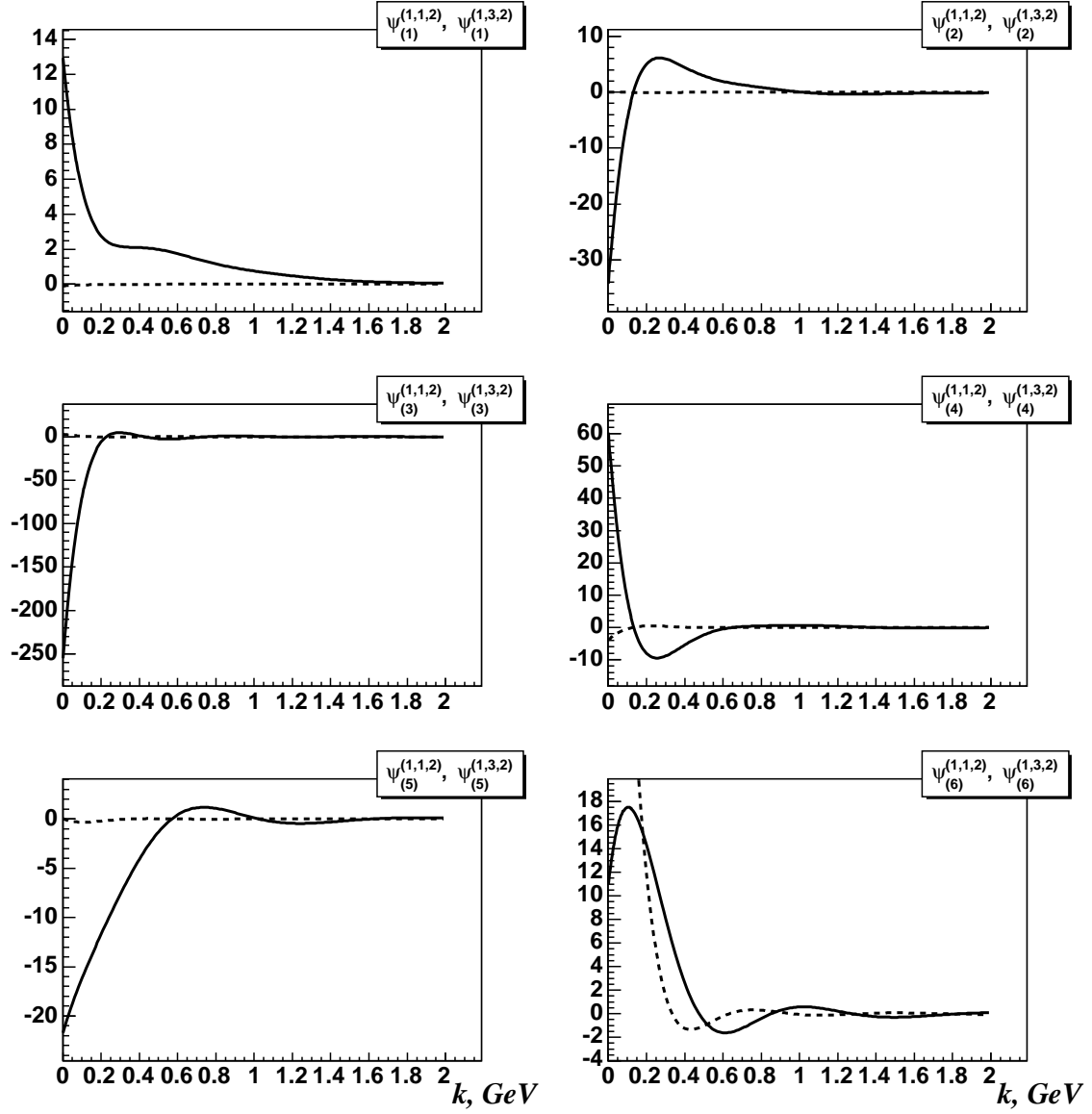


Figure 11: Wave functions for  $\chi_{b2}$  in the solution  $I(b\bar{b})$ . Solid and dashed lines stand for  $\psi^{(1,1,2)}$  and  $\psi^{(1,3,2)}$ .

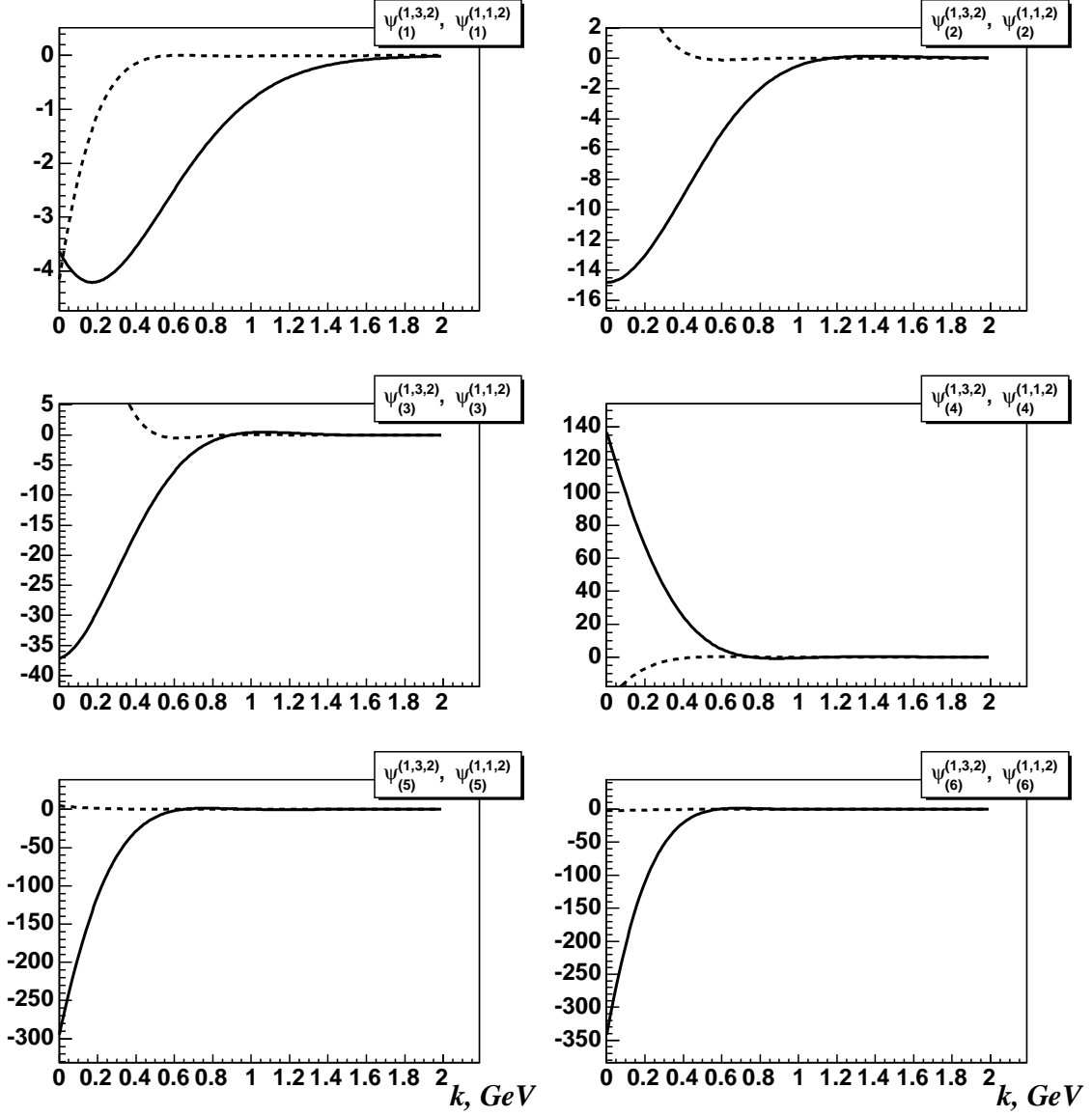


Figure 12: Wave functions for  $\chi_{b2}$  in Solution  $I(b\bar{b})$ . Solid and dashed lines stand for  $\psi^{(1,3,2)}$  and  $\psi^{(1,1,2)}$ .

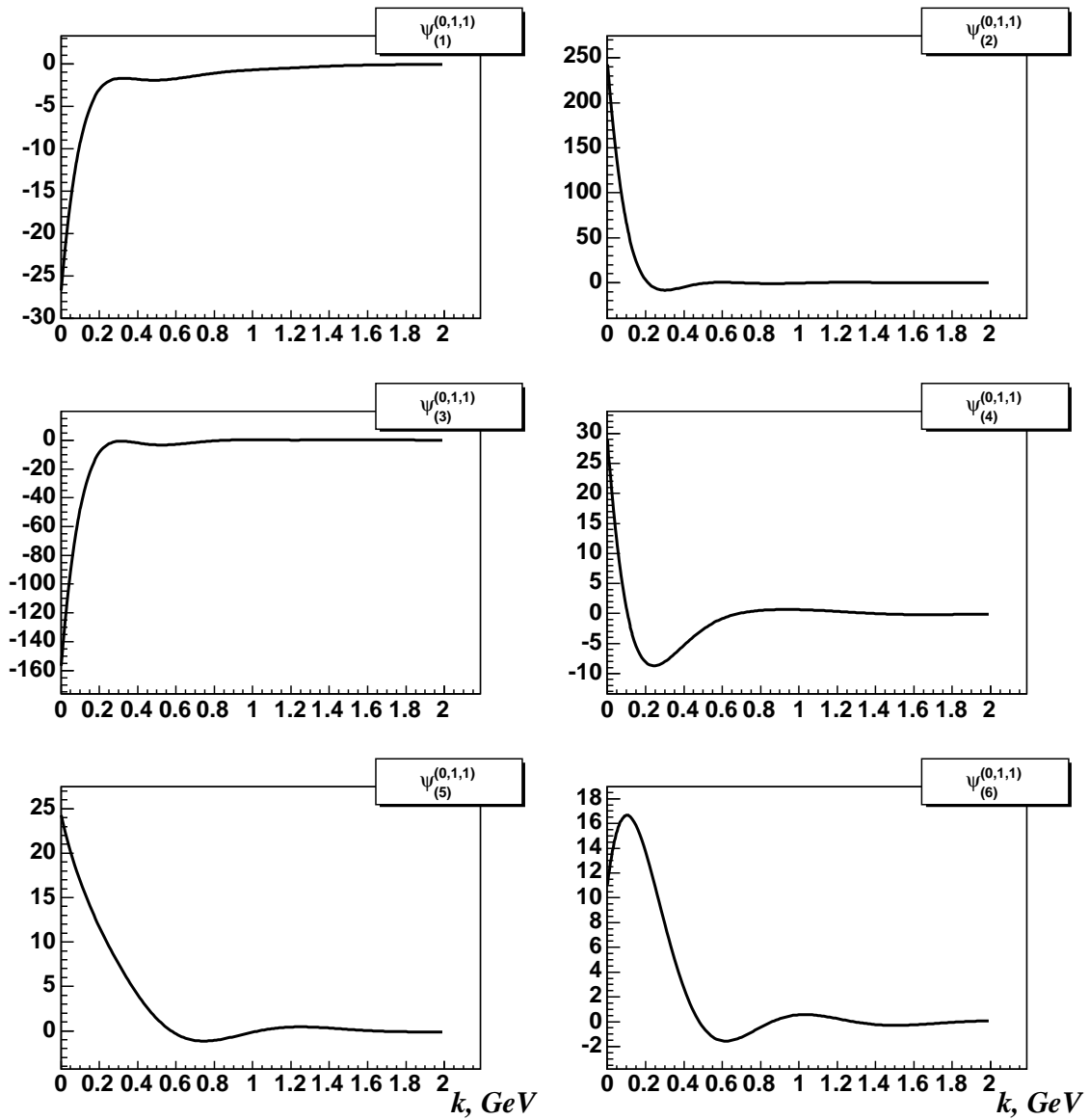


Figure 13: Wave functions for  $b_{b1}$  in the solutions  $I(b\bar{b})$ .